ELSEVIER

Contents lists available at ScienceDirect

Forest Ecology and Management

journal homepage: www.elsevier.com/locate/foreco



Long-term demography and stem productivity of Everglades mangrove forests (Florida, USA): Resistance to hurricane disturbance



Victor H. Rivera-Monroy^{a,*}, Tess M. Danielson^a, Edward Castañeda-Moya^b, Brian D. Marx^c, Rafael Travieso^b, Xiaochen Zhao^a, Evelyn E. Gaiser^b, Luis M. Farfan^d

- a Department of Oceanography and Coastal Sciences, College of the Coast and Environment, Louisiana State University, Baton Rouge, LA, USA
- b Department of Biological Science and Southeast Environmental Research Center, Florida International University, Miami, FL, USA
- ^c Department of Experimental Statistics, College of Agriculture, Louisiana State University, Baton Rouge, LA, USA
- d Centro de Investigación Científica y de Educación Superior de Ensenada, Unidad La Paz, Baja California Sur, Mexico

ARTICLE INFO

Keywords: Mangrove productivity Resistance Resilience Hurricane Florida Coastal Everglades Neotropics

ABSTRACT

Mangrove wetlands along coastal regions in neotropical northern latitudes are exposed to frequent hurricanes and therefore depend on resistant and resilient attributes to persist after these extreme events. However, few long-term studies have documented mangrove forest dynamics following hurricane disturbance to determine how species-specific phenotypic plasticity, species range shifts, and environmental stress interact to determine recovery trajectories. We present here a comprehensive analysis of Hurricane Wilma's (hereafter, "Wilma") impact (category 3, October 2005) on mangrove forest demography and aboveground net productivity in the Everglades, Florida (USA). We determined spatiotemporal patterns over a 15-year period (5 pre- and 10 post-Wilma) in three impacted sites on a productivity gradient along the Shark River Estuary. Hurricane resistance was evident in the low cumulative tree mortality and long-term recovery from defoliation (~10 years). Aboveground standing carbon stocks were not significantly reduced, as mortality ranged only from 3 to 10%. A negative linear relationship between Leaf Net Primary Productivity (NPP_L) and foliar residence time along the estuary shows that an increase in foliar production results in shorter residence time, which is defined by the interannual variation in NPP_L rates and recovery periods across sites. We propose this relationship as a proxy of canopy recovery in latitudinal comparative studies across mangrove ecotypes and coastal settings. This work advances ecological disturbance theory and ecological modeling of mangrove forests; specifically, we provide quantitative relationships among structural properties and dynamic processes to validate agent-based demographic and biogeochemical models to forecast the impact of natural and human disturbances on mangrove wetlands under climate change.

1. Introduction

Studies of population structure dynamics (e.g., demography) and productivity of mangrove forests are globally ubiquitous and reveal high spatial variability with complex drivers (Pool et al., 1977; Saenger and Snedaker, 1993; Sherman et al., 2003; Castañeda-Moya et al., 2013; Costa et al., 2015; Rovai et al., 2016; Osland et al., 2017; Rivera-Monroy et al., 2017; Osland et al., 2018; Rovai et al., 2018). These drivers of demographic and functional dynamics can be broadly characterized by slowly changing pressures, such as increasing temperature, sea level rise (i.e., presses) and disturbances such as storms, cold spells and lightning strikes/fires (i.e., pulses) that operate at different spatiotemporal scales (Collins et al., 2011; Becknell et al., 2015). Of these

drivers, hurricanes are a predictable feature in coastal regions in neotropical northern latitudes (Caribbean and Gulf of Mexico; Farfan et al., 2014; Simard et al., 2019), bringing high winds, heavy rain, and storm surges that cause canopy defoliation, tree mortality, and biochemical/geomorphological changes. Mangrove forests, therefore, have resistant and resilient attributes that allow them to persist after hurricanes, including species capable of ecophysiological responses that allow them to recover quickly when damaged by storms (Alongi, 2008; Lugo, 2008; Macamo et al., 2016; Rivera-Monroy et al., 2017; Imbert, 2018; Nehru and Balasubramanian, 2018; Servino et al., 2018).

Lightning strikes and hurricanes are the most common types of natural disturbances affecting mangrove forests structure in south Florida in the Gulf of Mexico, and are intense events causing significant

^{*} Corresponding author at: LSU Campus, Room 3209 Energy Coast and Environment Bldg., Baton Rouge, LA 70803, USA. E-mail address: vhrivera@lsu.edu (V.H. Rivera-Monroy).

defoliation and mortality (Smith et al., 1994; Doyle et al., 1995; Smith et al., 2009; Rivera-Monroy et al., 2011; Barr et al., 2012). High intensity hurricanes (i.e., category 3-5) are estimated to occur every 14-22 years in this region, but climate change is expected to potentially increase lighting strikes (Romps et al., 2014) and hurricane intensity (Gilman et al., 2008; Bhatia et al., 2018; Bhatia et al., 2019) and frequency (Knutson et al., 2010; Murakami et al., 2018). In south Florida, this trend was apparent with Hurricanes Donna (1960, category 4), Andrew (1992, category 5), and Wilma (2005, category 3) and the record setting number of storms during the 2005 and 2017 Atlantic hurricane season (Beven et al., 2008; Sun et al., 2008; Chao and Tolman, 2010; Zhang et al., 2016; Murakami et al., 2018). While a number of studies have been conducted to assess the impacts of these hurricanes (Baldwin et al., 2001; Milbrandt et al., 2006; Ross et al., 2006; Zhang et al., 2016), there are limited long-term studies quantitatively assessing disturbance magnitude and recovery patterns for multiple forest structural and functional variables.

A recent study along the southwest coast of the Florida Peninsula showed that mangrove litterfall net primary productivity (NPP_L) of mangrove stands impacted by Hurricane Wilma (2005, hereafter, "Wilma") had a differential resilience response to hurricanes related to disturbance magnitude and initial forest conditions (Danielson et al., 2017). After 5 years, sites located at the mouth and the middle along the estuary returned to pre-Wilma NPPL rates while others had not yet recovered (Danielson et al., 2017). Here, we examine productivity responses since this time, as well as the resilience patterns of other properties (i.e., stem, basal area, density) in the same sites. We define the resistant properties of the forest as the susceptibility of an ecosystem property to disturbance, or the ecosystem's ability to resist change (Bernhardt and Leslie, 2013; Becknell et al., 2015). This longterm dataset also allows us to quantify resilience, measured by rates of mortality and re-sprouting from defoliated tree trunks (e.g., Vogt et al., 2012; Shiels et al., 2015). By identifying the resistant components of a disturbance-prone ecosystem, we can quantitatively define their vulnerability and recovery trajectories.

Tree mortality caused by natural disturbances produce forest canopy openings of different dimensions including gaps and patches (McCarthy, 2001). Gaps are defined as "canopy openings not generally exceeding 200 m² usually caused by death of a single or group of trees, stem breakage due to root and butt diseases or windthrow in some cases" while patches are "larger openings (> 200 m²) induced by rapid, sometimes catastrophic, biotic and abiotic disturbances (e.g., fire, insect outbreak, hurricanes) (White and Pickett, 1985; McCarthy, 2001; Walker and De Moral, 2003; Busing et al., 2009; Frolking et al., 2009). These two conspicuous spatial patterns along a continuum are present in a surrounding forest matrix where they display clear structural and functional patterns (McCarthy, 2001). Although gap-patch dynamic theory has been informed by a number of studies in a variety of forests (McCarthy and Weetman, 2006; Busing et al., 2009), there is limited quantitative information from mangrove wetlands (e.g., Duke, 2001; Vogt et al., 2014) where hurricanes of different intensity can exert significant control in the role of gap and patches triggering a number of overlapping successional trajectories across the landscape (McCarthy, 2001; Lacambra et al., 2013). The limited long-term empirical studies assessing forest recovery in mangrove wetlands indicate that successional trajectories result from the interaction between species-specific phenotypic plasticity and species range shifts along environmental conditions partially influenced by gap and patch creation (Ball, 1980; Sherman et al., 2000; Duke, 2001; Zhang et al., 2008).

Although ecological modeling of gap dynamics and disturbance contributes to our understanding of how hurricane events modify the mechanisms controlling succession in forest gaps and patches (e.g., Busing and Mailly, 2004; Host et al., 2008), there are few mangrove wetland studies validating model conceptual frameworks and results (e.g., Berger et al., 2008); especially in cases when patch dynamics become dominant relative to the presence and density of forest gaps.

For instance, simulations in the KiWi and FORMAN models, developed for neotropical mangroves, show that disturbance response trajectories are indeed influenced by species interactions and abiotic conditions; particularly, soil fertility, salinity, and light gradients (Chen and Twilley, 1998; Twilley et al., 1998; Piou et al., 2008; Vogt et al., 2014). However, data from long-term empirical studies are necessary to directly evaluate the natural successional response to hurricane disturbance in both forest patches and gaps, and to verify and improve model simulations at different spatial scales (Busing and Mailly, 2004; Busing et al., 2009; Vogt et al., 2012; Shiels et al., 2015; Angeler and Allen, 2016)

This study is a comprehensive analysis of the spatiotemporal patterns of demography and aboveground productivity of mangrove forests in the Everglades before and after a major hurricane. Wilma was a high magnitude disturbance that crossed south Florida in late October 2005 and progressed into a category 3 storm moving from the Gulf of Mexico across the southern region of Everglades National Park (ENP) (Beven et al., 2008; Castañeda-Moya et al., 2010; Rivera-Monroy et al., 2011; Danielson et al., 2017) (Fig. 1). We used baseline (pre-Wilma: 2000-2004) forest properties (e.g., density, stem productivity) to quantitatively evaluate hurricane impact (immediate-post-Wilma: 2006-2009) and forest recovery (post-Wilma: 2011-2015) to address the following questions: (1) Do basal area, tree density, and aboveground biomass change as result of Wilma's impact? were all species and/or size classes affected at the same level? (2) How did variation in defoliation and mortality affect stem net primary productivity (NPPs)? (3) What forest structural properties exhibit resistance, and how do these properties contribute to forest recovery trajectories? Our analysis identifies the uncertainties in disturbance theory and defines the role of resilience and resistance in maintaining mangrove forest properties in the long term in this coastal region.

2. Methods

2.1. Study site

The Florida Coastal Everglades Long Term Ecological Research (FCE LTER) program established two landscape-level transects where permanent plots were established in Dec-2000 at two main coastal drainage basins: Shark River Slough (Fig. 1) and Taylor Slough. The mangrove-dominated forest sites in the Everglades mangrove ecotone region (hereafter Everglades) (Rivera-Monroy et al., 2011) along the Shark River Estuary (SRS) are SRS-4 (18.2 km from the mouth), SRS-5 (9.9 km), and SRS-6 (4.1 km). These sites undergo minimum direct human disturbance (e.g. deforestation) but are indirectly affected by upstream hydrological changes as part of the Comprehensive Everglades Restoration Plan (Sklar et al., 2005; Rivera-Monroy et al., 2011). There are well defined fertility, salinity, and hydrologic gradients along the SRS where total phosphorous (0.05 to $0.20 \,\mathrm{mg}\,\mathrm{cm}^{-3}$), salinity (4 to 26 ppt), and hydroperiod (3695 to 5592 hr yr⁻¹, 217 to 395 tides yr⁻¹) increase towards the mouth of the estuary (Chen and Twilley, 1999; Castañeda-Moya et al., 2013). Tree height also increases with distance towards the mouth of the estuary and average height range is from 5 to 15 m (Simard et al., 2006). Significant differences in soil pore water conditions and NPP₁ are also caused by distinct dry (December-May) and wet (June-November) seasons. The sites SRS-4 and SRS-5 are dominated by the species Rhizophora mangle, while SRS-6 is dominated by Laguncularia racemosa. Other species present at these sites include Avicennia germinans and Conocarpus erectus (Castañeda-Moya et al., 2013).

2.2. Experimental design

In 2000, two 20 \times 20 m permanent plots were established in SRS-4, SRS-5, SRS-6. Within each plot, all trees with a diameter at breast height (DBH) \geq 2.5 cm were tagged and species registered.

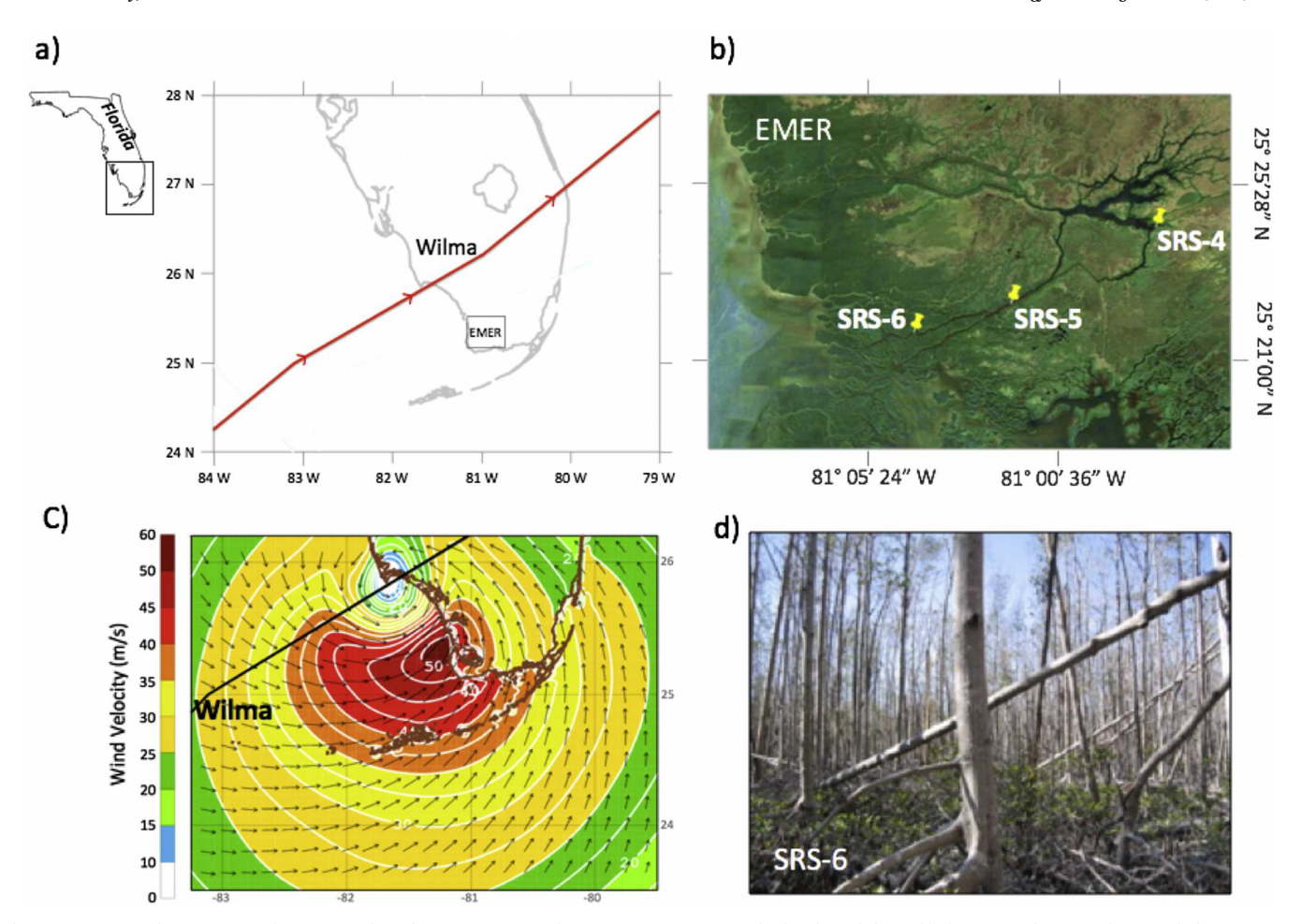


Fig. 1. Site map and Hurricane Wilma (2005) disturbance event. a) Wilma trajectory across south Florida and the Gulf of Mexico relative to the Everglades mangrove ecotone region (EMER); (b) FCE LTER sites SRS-4, SRS-5 and SRS-6 locations; (c) Wilma wind field (speed in m s⁻¹) and storm path (black line); the wind field analyses were obtained from the legacy archive provided by Hwind at https://hwind.co and the path from the National Hurricane Center records available at https://www.nhc.noaa.gov/); (d) Photo of Hurricane Wilma impact at the SRS-6 site (*Photo credit: Victor H. Rivera-Monroy, 12-Dec-2005*).

Measurements occurred on an annual or biennial basis in the years 2000, 2001, 2002, 2003, 2004, 2006, 2008, 2009, 2011, 2013, and 2015. Due to initial field sampling conditions, only plot #1 was surveyed in 2000 and only plot #2 was surveyed in 2001 at all sites. Beginning in year 2002, two plots (considered here the experimental unit) were systematically sampled. DBH histograms (stem frequency per size class) were plotted for each site and year to analyze moment parameters (mean, variance, skewedness, kurtosis) of the density distribution probability curve. Total area under the distribution curve was also used to determine DBH changes over time. A tree height survey for all species was conducted in 2003 in each plot. Pre (2000-2004), Immediate-Post (2006-2009) and Post (2011-2015) categories were assigned to test for temporal variations in forest structure as related to Wilma's impact in 2005. The temporal range of these categories was adjusted for breakpoint linear regression and the mortality assessment as defined below.

The forest structure variables included in the analysis were: mortality, species composition, species dominance, basal area ($\rm m^2~ha^{-1}$), and tree density (stems $\rm ha^{-1}$) by DBH size classes. These variables were used to calculate the forest complexity index (CI) for comparative purposes (Holdridge et al., 1971). Tree mortality was defined as the number of dead trees divided by the total number of live trees from the previous year. Trees were categorized into size classes based on DBH starting at 2.5–5 cm and increasing at 5 cm intervals to a maximum value of 40 cm. If the tree outgrew the initial size class, it was reassigned to a new size class. CI was calculated for all sites using the following equation (Holdridge et al., 1971):

 $CI = Stem Height \times Basal Area \times Stem Density \times number of species \times 10^{-5}$

In situ species-specific allometric equations for R. mangle, A. germinans, and L. racemosa were used to calculate the aboveground biomass (AGB) for both leaf and stem wood components of each tagged tree within the plots (Smith and Whelan, 2006). For C. erectus, the L. racemosa equation was also used because of the similar growth form between these two species (Chen and Twilley, 1999). Only total AGB and leaf biomass equations were calculated and used in this study; wood AGB was determined as the difference between total and leaf biomass. The annual, or biennial net increase in wood biomass was calculated as the difference in wood AGB between sampling dates for each individual tree. The stem net primary productivity (NPPs) was calculated as the sum of net increase for each plot; site NPPs was estimated as the mean of the two plots (i.e., experimental units).

Aboveground biomass (AGB) "anomalies" per site and component were estimated as the percent change in AGB from initial AGB estimates, where initial AGB was the mean of the AGB value for the period 2000-2001 (AGB $_{2000-2001}$). We used AGB $_{2000-2001}$ to include the initial AGB from plot 1 (2000) and plot 2 (2001). This anomaly approach was used to define distinct temporal changes in AGB from the baseline pre-Wilma conditions (2000–2001). Foliar residence time (yr) was calculated by dividing the leaf biomass by the total leaf litterfall net primary productivity (leaf NPP_L) previously obtained by (Danielson et al., 2017) Foliar residence time was calculated only for the years when both litterfall productivity (NPP_L) and leaf AGB data were available (2002–2004, 2006, 2008, 2009, 2011, 2013).

2.3. Statistical analysis

All statistical analyses were performed using SAS software (SAS Institute, Cary, NC, USA). For all sites, a breakpoint linear regression model was fit for DBH area under the curve vs. time (2002-2015) and compared the model for differences between hurricane periods: pre-Wilma (2000–2004) and post-Wilma (2006–2015). The breakpoint (C) year = 2005. model set The general at $Y = \beta 0 + \beta 1(X) + \beta 2(X - C) + \varepsilon$ where β_0 is the intercept, β_1 is the slope before 2005, β_2 is the difference from the 2005 slope. If the β_2 parameter is significant, the pre and post-Wilma slopes are significantly different indicating changes in structural attributes due to Wilma's impact. Site-specific moment parameters (mean, variance, skewedness, kurtosis) were also obtained using linear regression and breakpoint analyses to compare 2000-2004 and 2006-2015 period slopes.

Two-way analysis of variance (ANOVA) models were used to test for significant differences among Wilma periods (pre, immediate-post, post) and SRS sites. This model was used to evaluate significant changes in mortality, BA, density, AGB, NPP_S, and foliar residence time. Sites and Wilma periods were considered random effects and plot was considered the experimental unit. Linear regressions were performed for residence time vs. leaf NPP_L and vs. Leaf AGB data. Additionally, site-specific linear regression equations were also obtained for the residence time vs. leaf NPP_L analysis. These site-specific regressions excluded the year 2006 values, which represented the immediate effect of Wilma. Difference in slopes among models was evaluated using a mixed model.

Since resistance implies no change in an ecological response as result of a disturbance (Pickett et al., 1989; White and Jentsch, 2001; Busing et al., 2009; Bernhardt and Leslie, 2013; Seidl et al., 2017; Lucash et al., 2018), the alternative hypothesis was a test for Hurricane effect, where this type of disturbance will have a significant impact on both structural and functional variables. The null hypothesis states that the mean value for all variables was the same for the three periods considered in the two-way ANOVA analysis (i.e., pre-Wilma, immediate-post Wilma and post-Wilma). Thus, if no significant difference is observed when comparing the pre-Wilma period against both the immediate and post-Wilma periods, then it would indicate that the variable was resistant to hurricane impacts (i.e., no ecological change). A variation to this outcome occurs when the pre-Wilma period is significantly different than the immediate-post period, but not to the post-Wilma period, signaling that the variable changed due to the hurricane impact in the short-term (i.e., immediate period), but eventually reached the original (i.e. pre) values in the long-term (post-period) as result of its resilience capacity.

3. Results

3.1. Structural impact

There was a differential impact on forest structure by Wilma across study sites. Forest structure at each site was first characterized using DBH histograms for each site (Fig. S1). Initial (2002) DBH distribution was skewed towards trees of smaller class sizes (2.5–10 cm) at SRS-4, while trees at SRS-5 and SRS-6 were more evenly distributed across a larger range (2.5–45 cm). The regression analysis showed that DBH total area varied significantly over time in the SRS-6 site only (P = 0.0005), such that the overall area under the curve decreased after 2005 (Table 1). However, there were significant changes in DBH over time in SRS-4 Plot 1 (P = 0.005), SRS-5 Plot 2 (P = 0.0153) and in both plots at SRS-6, indicating local spatial variability in forest structure at each site. For all sites, DBH distribution moment parameter analysis showed that there was no significant change in skewedness or kurtosis over time at all sites (P > 0.05) (Table 1).

Mortality varied across sites and Wilma time periods where pre-Wilma (2002–2004) mortality was < 3% at all sites (Fig. S2). The SRS-6 site had the greatest immediate-post-Wilma (2006) mortality (15%)

Table 1 Breakpoint linear regression summary for diameter at breast height (DBH) area, DBH skewedness, and DBH kurtosis site-specific models. The breakpoint (C) was set at year = 2005. Model: $Y = \beta 0 + \beta 1(X) + \beta 2(X - C)$ where β_0 is the intercept, β_1 is the slope before the 2005, β_2 is the difference from 2005 slope. ns = not significant.

Model	βο	β_1	β_2	R ² Model	F Value	P Model		
DBH Area								
SRS-4	-52602	26.7 ^{ns}	-27.00^{ns}	0.4173	$F_{(3,7)} = 1.67$	0.2589		
SRS-5	-12467	6.7 ^{ns}	-5.63 ^{ns}	0.5817	$F_{(3,7)} = 3.24$	0.0904		
SRS-6	16,939	-7.8^{ns}	-36.54^{ns}	0.9076	$F_{(3,7)} = 22.9$	0.0005		
DBH Skev	DBH Skewedness							
SRS-4	65.9	-0.032^{ns}	0.027^{ns}	0.7596	$F_{(3,7)} = 7.37$	0.0143		
SRS-5	-11.9	0.06 ^{ns}	-0.064^{ns}	0.3337	$F_{(3,7)} = 1.17$	0.3875		
SRS-6	-24.3	0.013 ^{ns}	0.001 ^{ns}	0.1662	$F_{(3,7)} = 0.47$	0.7157		
DBH Kurtosis								
SRS-4	322	-284^{ns}	0.14 ^{ns}	0.3830	$F_{(3,7)} = 1.45$	0.3082		
SRS-5	-1152	0.578 ^{ns}	-0.629^{ns}	0.2838	$F_{(3,7)} = 0.92$	0.4771		
SRS-6	49.2	-0.023^{ns}	0.021 ^{ns}	0.0498	$F_{(3,7)} = 0.12$	0.9440		

compared to the SRS-5 (3.5%) and SRS-4 (6%) sites. Post-Wilma (2008–2015) mortality remained higher than pre-Wilma mortality across all sites, especially in SRS-6 (9%) (Fig. S2).

Total basal area (BA) was significantly higher (P = 0.0003) downstream at the SRS-6 site and decreased upstream at the SRS-5 and SRS-4 sites (Fig. S3). There were temporal variations in BA magnitude, although the spatial trend was not as pronounced by 2015. At SRS-6, total BA (i.e., all species) was $41.2 \pm 4.2 \,\mathrm{m^2} \,\mathrm{ha^{-1}}$ in the pre-Wilma period and decreased by 28% to $29.8 \pm 2.6 \,\mathrm{m^2} \,\mathrm{ha^{-1}}$ in the post-Wilma period (Fig. S3). At SRS-5, BA increased by 5% from pre- ($20.6 \pm 1.3 \,\mathrm{m^2} \,\mathrm{ha^{-1}}$) to post-Wilma ($21.6 \pm 2.1 \,\mathrm{m^2} \,\mathrm{ha^{-1}}$). Similarly, SRS-4 total BA increased by 10% from the pre- ($23.4 \pm 4.1 \,\mathrm{m^2} \,\mathrm{ha^{-1}}$) to the post-Wilma period ($25.7 \pm 4.1 \,\mathrm{m^2} \,\mathrm{ha^{-1}}$). Relative species contribution to total BA at each site did not shift (Fig. S3) over the 15-year period considered in this analysis. *L. racemosa* showed the greatest contribution to SRS-6 total BA (50-55%), while *R. mangle* had the greatest contribution to SRS-5 (83%) and SRS-4 (50%) (Fig. S3).

Total (all trees with DBH > 2.5 cm) stem density was significantly greater (P < 0.0001) at SRS-4 (7593 \pm 120) than at SRS-5 (2792 \pm 34) and SRS-6 (2453 \pm 142) (Fig. 2, Table 2), particularly in the 2.5–5 cm size class. This tree density difference was consistent throughout the sampling period (2000–2015). Additionally, no significant difference (P > 0.05) in total stem density was registered among hurricane periods. The relative size class density did not shift over time; the highest stem density in SRS-4 occurred in the 2.5–5 cm size class and in the 5–10 cm DBH size class in both SRS-5 and SRS-6. Pre-Wilma density of smaller trees (< 10 cm) decreased downstream from 6750 stems ha $^{-1}$ at SRS-4 to 1434 stems ha $^{-1}$ at SRS-6. Pre-Wilma density of larger trees (> 10 cm) increased downstream from 615 stems ha $^{-1}$ at SRS-4 to 1488 stems ha $^{-1}$ at SRS-6 (Fig. 2).

Tree density at SRS-4 was skewed towards smaller size classes, and density decreased with an increase in size class, which ranged from 2.5 to 20 cm. *R. mangle* had the highest tree density at this site, but *L. racemosa* had the greatest density within the 10–15 cm size class, while *C. erectus* stems dominated the 15–20 cm size class. From pre-(2000–2004) to post-Wilma (2011–2015) there was a 10% overall reduction in total density at SRS-4, but the stem density of larger trees (10–40 cm size class) increased by 60% and density of smaller trees (2.5–5 cm) decreased by 15%. Total density at SRS-5 was only reduced by 2% from pre- to post-Wilma (2862 \pm 613 to 2794 \pm 2793 stems ha $^{-1}$) (Table S1 Supplementary). A reduction in smaller trees (7%) and an increase (6%) in larger trees from pre- to post-Wilma was observed, similar to the pattern observed in SRS-4. *R. mangle* was the dominant species in SRS-5 with the greatest density across all size classes. There was a notable increase in *L. racemosa* in the 2.5–5 cm size class from

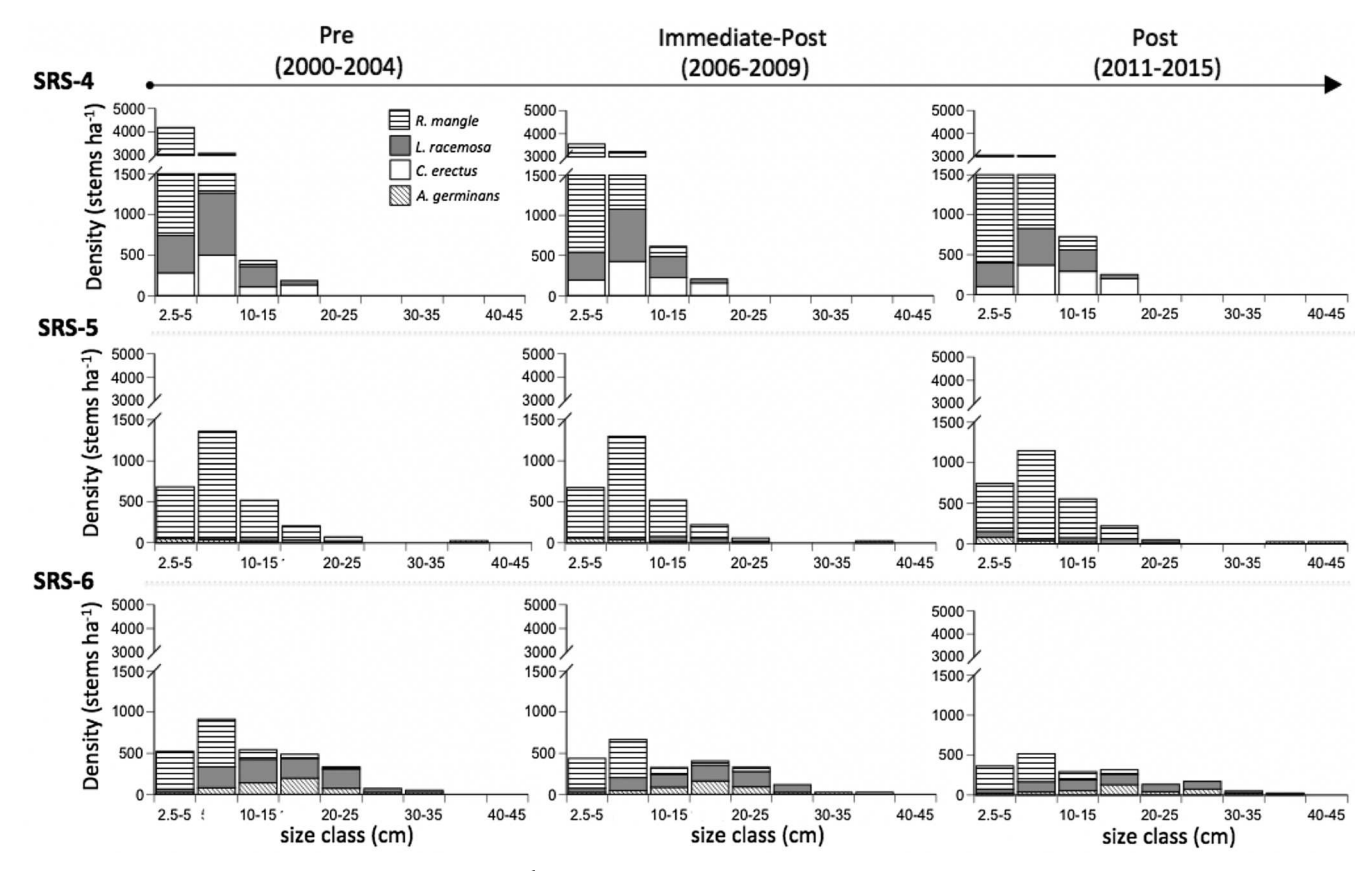


Fig. 2. Species-specific stem density (stems ha⁻¹) per size class (cm) for each site and hurricane period (Pre-, Immediate-Post, Post).

pre- to post-Wilma (0 to 75 stems ha $^{-1}$) (Fig. 2). At SRS-6, density was evenly distributed across size classes; 1434 stems ha $^{-1}$ for smaller trees and 1488 stems ha $^{-1}$ for larger trees. *R. mangle* dominated the 2.5–10 cm DBH size class, but *L. racemosa* had the greatest relative density in larger size classes, and was the dominant species in the site overall. There was a 36% reduction in total density from pre-to post-Wilma (2921 \pm 640) to 1866 \pm 267 trees ha-1), where all size class densities were evenly reduced (Table S1 Supplementary).

A significant site effect (P < 0.05) for AGB in both wood and leaf components were detected. In this case, SRS-5 total AGB was significantly less than SRS-6 (Fig. 3a), but there was no significant annual effect or site by year interaction (Table 3). The mean total AGB (\pm SE) (Mg C ha $^{-1}$) from 2000 to 2015 was 54 (\pm 1.3) in SRS-4, 45 (\pm 0.51) in SRS-5, and 66 (\pm 3.1) in SRS-6 (Fig. 3a). At SRS-4 and SRS-5 total AGB from pre (2000–2004) to post (2011–2015) Wilma increased by < 12%. At SRS-6 there was a 27% decrease in AGB from pre to post-Wilma, which resulted in a post-Wilma AGB magnitude (53.5 Mg C ha $^{-1}$) similar to SRS-4 (56.5 Mg C ha $^{-1}$). (Table S2 Supplementary).

The AGB anomalies from initial conditions (AGB₂₀₀₀₋₂₀₀₁) for leaf and wood components showed annual and site variation (Fig. 3b). Anomalies within \pm 5% were considered normal inter-annual variability. At SRS-4 anomalies ranged from 3 (2002) to 25 (2014) percent while SRS-5 showed a range of -6 (2009) to 6% (2015) departure from AGB₂₀₀₀₋₂₀₀₁ including temporal differences in both wood and leaf biomass components. At SRS-6, AGB anomalies ranged from -35 (2015) to 8% (2005) and negatively increased with time after Wilma impact (2005) (Fig. 3b).

The forest complexity index (CI) was distinct among sites in the pre-Wilma period, where SRS-6 had the highest CI (46.6), and SRS-5 had the lowest (14.7) (Fig. 4); this index was estimated by using the product of a number of structural attributes that are generally impacted by storms (see methods). After Wilma, the CI did not shift in sites SRS-4 and SRS-5. However, in SRS-6, the CI decreased first to 33.4 immediate-post-Wilma, then further declined to 21.3 post-Wilma. The final SRS-6 CI was a value closer to the SRS-5 CI at the post-Wilma period (Fig. 4).

Table 2 Summary of site and hurricane period (Pre: 2000–2004; Immediate-Post: 2006–2009, Post: 2011–2015) means (\pm SE) for the variables Basal Area (m² ha⁻¹), Stem Density (stems ha⁻¹), Aboveground Biomass (Mg C ha⁻¹), Stem Net Primary Productivity (Mg C ha⁻¹ yr⁻¹), and Residence Time (yr). Different lower-case letters indicate significant differences among sites and hurricane period means.

	Stem Density	Aboveground Biomass	Stem Net Primary Productivity	Residence Time
$m^2 ha^{-1}$	Stems ha ⁻¹	Mg C ha ⁻¹	$Mg C ha^{-1}yr^{-1}$	yr
$8.27 (0.62)^a$	7593 (120) ^a	54 (1.13) ^{ab}	1.17 (0.11) ^a	$0.85 (0.10)^a$
6.98 (0.90) ^a	2792 (34) ^b	45 (0.51) ^b	0.74 (0.05) ^b	0.56 (0.09) ^b
12.16 (0.93) ^b	2453 (142) ^b	66 (3.11) ^a	1.49 (0.10) ^a	0.40 (0.09) ^c
9.47 (0.89) ^a	3897 (807) ^a	56 (3.5) ^a	1.22 (0.18) ^a	$0.52 (0.05)^a$
9.25 (0.92) ^a	4263 (8 6 1) ^a	56 (3.4) ^a	$1.06 (0.07)^a$	$0.80 (0.15)^{b}$
8.57 (0.77) ^a	4518 (6 2 9) ^a	52 (1.7) ^a	1.06 (0.09) ^a	0.46 (0.09) ^a
	8.27 (0.62) ^a 6.98 (0.90) ^a 12.16 (0.93) ^b 9.47 (0.89) ^a 9.25 (0.92) ^a	8.27 (0.62) ^a 7593 (120) ^a 6.98 (0.90) ^a 2792 (34) ^b 12.16 (0.93) ^b 2453 (142) ^b 9.47 (0.89) ^a 3897 (8 0 7) ^a 9.25 (0.92) ^a 4263 (8 6 1) ^a	8.27 (0.62) ^a 7593 (120) ^a 54 (1.13) ^{ab} 6.98 (0.90) ^a 2792 (34) ^b 45 (0.51) ^b 12.16 (0.93) ^b 2453 (142) ^b 66 (3.11) ^a 9.47 (0.89) ^a 3897 (8 0 7) ^a 56 (3.5) ^a 9.25 (0.92) ^a 4263 (8 6 1) ^a 56 (3.4) ^a	8.27 (0.62) ^a 7593 (120) ^a 54 (1.13) ^{ab} 1.17 (0.11) ^a 6.98 (0.90) ^a 2792 (34) ^b 45 (0.51) ^b 0.74 (0.05) ^b 12.16 (0.93) ^b 2453 (142) ^b 66 (3.11) ^a 1.49 (0.10) ^a 9.47 (0.89) ^a 3897 (807) ^a 56 (3.5) ^a 1.22 (0.18) ^a 9.25 (0.92) ^a 4263 (861) ^a 56 (3.4) ^a 1.06 (0.07) ^a

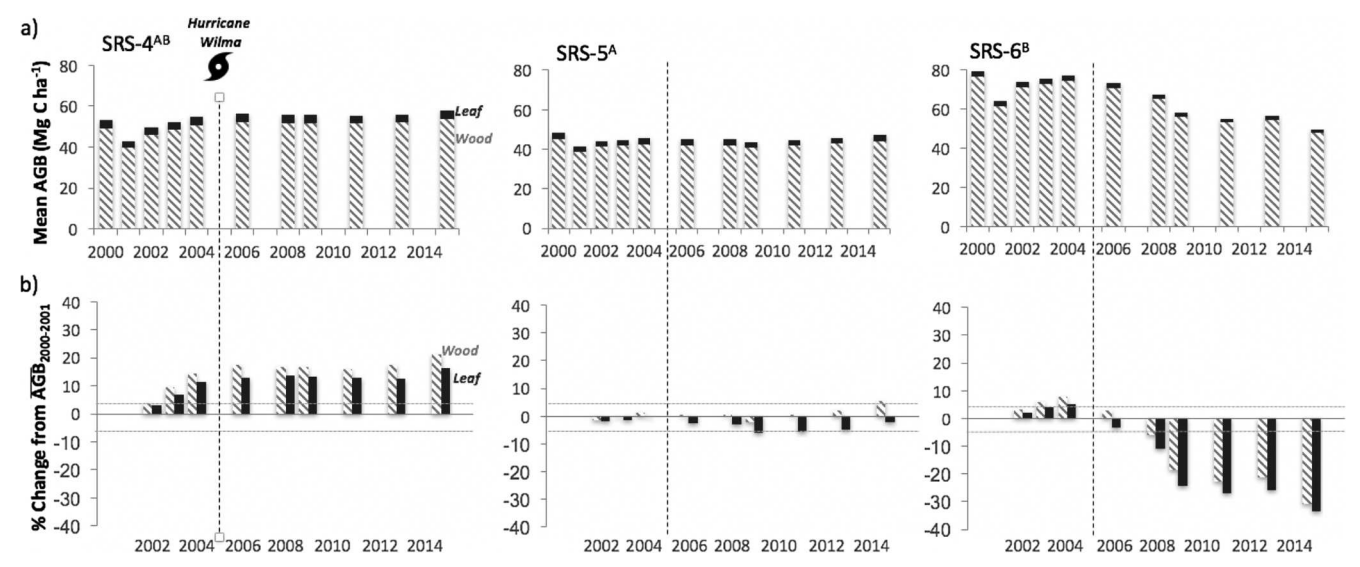


Fig. 3. (a) Mean annual above ground biomass (AGB, Mg C ha⁻¹) of leaf and wood components for each site during 2000–2015. (b) AGB anomalies from the initial (2000–2001 mean; AGB₂₀₀₀₋₂₀₀₁) for leaf and wood components. Horizontal lines at ± 5% show pre-Hurricane Wilma (cyclone symbol 6) variability range.

3.2. Forest functional patterns

Stem net primary productivity (NPP_S) varied significantly across sites (P < 0.001) (Fig. 5). At SRS-6, the 2000 to 2015 average value was 1.53 \pm 0.38 Mg C ha $^{-1}$ yr $^{-1}$ and significantly higher than in SRS-5 (0.73 \pm 0.18 Mg C ha $^{-1}$ yr $^{-1}$) and SRS-4 (1.15 \pm 0.34 Mg C ha $^{-1}$ yr $^{-1}$). Species-specific contribution to total NPP_S was greatest for *R. mangle* in SRS-4 and SRS-5, and *L. racemosa* in SRS-6. There was a change in stem productivity rates from pre-to post-Wilma periods in all sites, but it was not significant (P > 0.05) (Table S3 Supplementary); relatively, NPP_S decreased by 29% at SRS-4, increased by 55% at SRS-5, and decreased by 22% at SRS-6 from the pre to the post-Wilma period.

Foliar residence time was significantly different among sites (P < 0.001) and hurricane periods (P < 0.001) (Fig. 6, Table 3). At all sites, immediate-post-Wilma residence time was significantly longer compared to pre and post-Wilma. SRS-6 residence time was the shortest (0.35 yr, pre; 0.27 yr, post) followed by SRS-5 (0.51, pre; 0.44 post), then SRS-4 (0.7, pre; 0.79, post) (Fig. 6a). There was a positive linear relationship between Leaf AGB anomalies (2000–2001 baseline) and residence time ($R^2 = 0.31$, P = 0.0045, N = 42) (Fig. 6b). Conversely, the relationship between Leaf NPP_L vs residence time including data from all sites and years showed a negative linear relationship ($R^2 = 0.88$, P < 0.0001, N = 39) (Fig. 7a); when assessing this relationship per site excluding year 2006, right after Wilma impact, only the SRS-6 slope was not significant (P = 0.203) (Fig. 7b).

4. Discussion

Previous studies have shown that hurricane disturbance in the ENP and south Florida has significantly altered mangrove forest structure and function due to high mortality (Baldwin et al., 1995; Ross et al., 2006; Doyle et al., 2009; Smith et al., 2009). Yet, there is a lack of

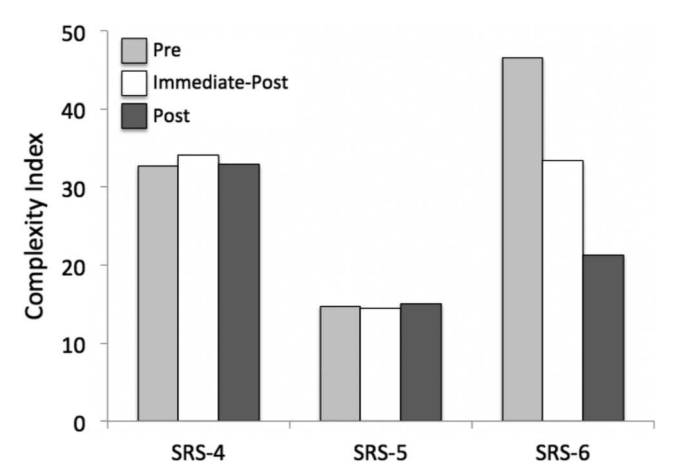


Fig. 4. Complexity index value (CI = Stem Height \times Basal Area \times Stem Density \times number of species \times 10⁻⁵) for each site at each hurricane impact period. Pre (2000–2004), immediate-post (2006–2009), post (2011–2015).

studies that quantify the interaction among disturbance and forest properties over long periods and that have a record of pre-disturbance conditions for long-term comparison (e.g., Doyle et al., 2009). Our study quantitatively demonstrates that structural variables (basal area, density, above-ground biomass) and NPP_S were not immediately changed by the storm, indicating resistance properties. Furthermore, by sampling along an exposure and productivity gradient, we discovered significant spatial variability in defoliation and mortality that influenced forest recovery in time-scales of less than a decade.

Table 3 Summary of F statistics for Basal Area (BA), Stem Density (Density), Aboveground Biomass (AGB), Stem Net Primary Productivity (NPP_S), and residence time ANOVA models. Significance is indicated by *P < 0.05, **P < 0.01, ***P < 0.0001, ^{ns}P > 0.05. Site effect levels are SRS-4, SRS-5, SRS-6, Hurricane effect levels are Pre, Immediate-Post, and Post.

ANOVA Source	BA	Density	AGB	NPP_S	Residence Time
Site Hurricane Site*Hurricane	$\begin{split} F_{(2,9)} &= 23.52^{*^{\circ}} \\ F_{(2,9)} &= 0.78^{ns} \\ F_{(4,9)} &= 1.9^{ns} \end{split}$	$\begin{split} F_{(2,708)} &= 68.6^{***} \\ F_{(2,708)} &= 0.92^{ns} \\ F_{(4,708)} &= 0.09^{ns} \end{split}$	$\begin{split} F_{(2,171)} &= 3.46^{\circ} \\ F_{(2,171)} &= 0.23^{ns} \\ F_{(4,171)} &= 0.62^{ns} \end{split}$	$\begin{aligned} F_{(2,11)} &= 11.84^{**} \\ F_{(2,11)} &= 1.22^{ns} \\ F_{(4,11)} &= 2.54^{ns} \end{aligned}$	$\begin{split} F_{(2,42)} &= 21.22^{***} \\ F_{(2,42)} &= 23.42^{***} \\ F_{(2,42)} &= 0.5^{ns} \end{split}$

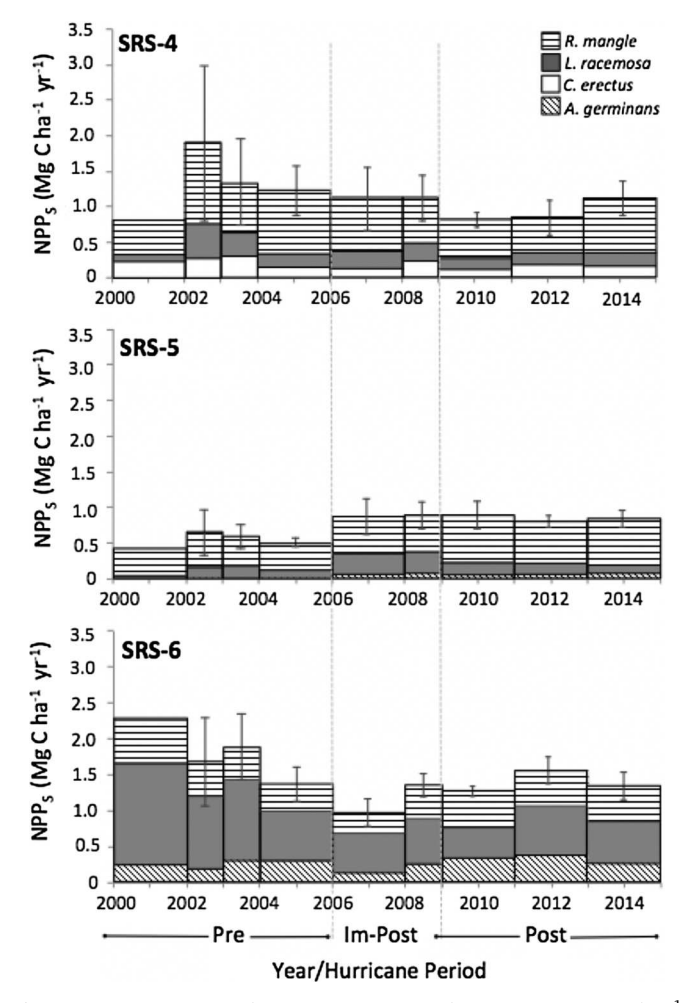
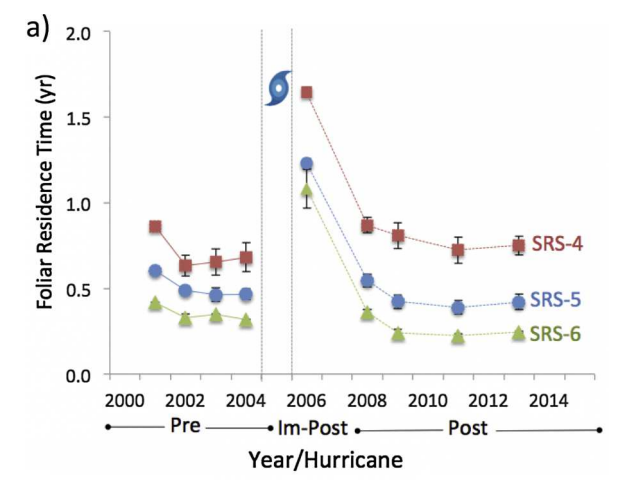


Fig. 5. Mean (\pm SE) annual stem net primary productivity (NPPs, Mg C ha $^{-1}$ yr $^{-1}$) per species for each mangrove site.

4.1. Structural properties

Stem mortality and recruitment are key regulators of mangrove structure and forest development. In the Everglades, mangrove mortality is frequently caused by lightning strikes and hurricane force winds (Doyle et al., 1995; Zhang et al., 2008; Whelan et al., 2009). During Wilma, wind speeds reached up to 45 m s⁻¹ (Fig. 1), yet stem mortality was low (i.e., immediate-post period Table 2; Fig. S2). Wilma's wind speeds were highest near the estuary mouth (Fig. 1), and caused the highest immediate mortality (15%). Continued delayed high mortality rates post-Wilma (9%) suggests that a portion of the defoliated trees at this site were unable to recover and eventually died within 2 years after impact, but overall these results suggest that mangrove structure was resistant to Wilma. Previous studies of hurricane-induced mortality in tropical forests found that the degree of exposure (i.e., distance from hurricane eye-wall, tree height) and storm intensity (i.e., wind velocity) causes spatial variability of forest impact (Baldwin et al., 1995; Milbrandt et al., 2006; Lacambra et al., 2013). Therefore, the relative mortality among mangrove stands is attributed partially to the differential wind speeds impact at each site (Danielson

Spatial differences in recovery among forest stands was obvious, particularly in the contrasting patterns of the upstream and downstream estuary sites. The AGB and BA increased from pre- to post-Wilma periods in the most upstream site (SRS-4), but decreased toward the mouth (SRS 6) (Fig. S3). Initially, SRS-4 and SRS-6 had distinctly different forest structure, where SRS-4 had a low BA and AGB values



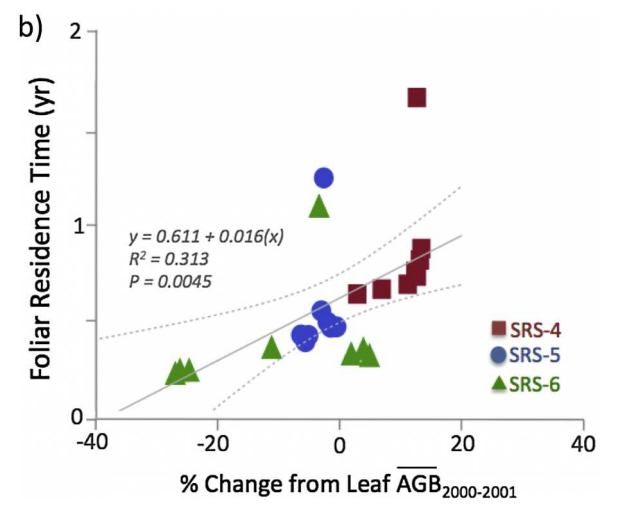


Fig. 6. (a) Mean (± SE) foliar residence time (yr) in Shark River estuary mangrove sites from 2001 to 2013. Hurricane symbol denotes Hurricane Wilma impact. (b) Linear regression of foliar residence time (yr) and Leaf AGB anomaly (% change from 2000 to 2001 Leaf AGB mean) across all sites.

and high density. In contrast, SRS-6 had high BA and AGB values and a low density. After Wilma, SRS-6 total stem density, AGB and BA values decreased due to higher cumulative mortality (Figs. 2, 3; Fig. S3). At SRS-4, lower mortality, tree growth, and higher recruitment resulted in both AGB and BA increase post-Wilma. Although total density decreased by 10% post-Wilma, there was a 60% increase in higher C. erectus and R. mangle densities and 15% decrease in smaller tree density (Fig. 2). These temporal patterns indicate that smaller trees were recruited to larger size classes thus contribution to higher AGB and BA values. Tree recruitment dynamics in SRS-4 resulted in a more similar BA value between SRS-4 $(25 \, \text{m}^2 \, \text{ha}^{-1})$ and SRS-6 $(29 \, \text{m}^2 \, \text{ha}^{-1})$ in the post-Wilma period, as opposed to the pre-Wilma period where BA values were twice as high in SRS-6 relative to SRS-4 (Castañeda-Moya et al., 2013). Yet, throughout the study period, SRS-4 tree density continued to be significantly higher than SRS-6, demonstrating the close relationship between tree size class, the initial number of trees, and forest total BA.

The AGB anomalies estimated using forest structure from the pre-Wilma period clearly indicate the annual departure (%) from the initial AGB values and underscore majors site differences in AGB trajectories (Fig. 3b). In SRS-5, anomalies only ranged between -6 and 6%, suggesting that long-term annual AGB had little variation from the pre-Wilma initial conditions. Furthermore, SRS-5 AGB anomalies showed that there was no significant change post-Wilma in this site. Thus,

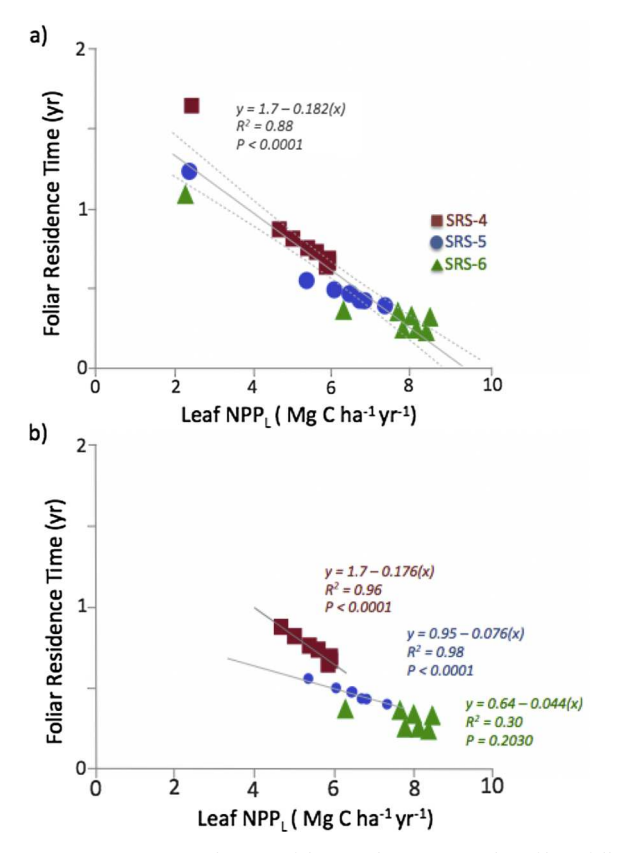


Fig. 7. (a) Linear regression between foliar residence time and Leaf litterfall net primary productivity (Leaf NPP_L) across all sites. (b) Site-specific linear regression between residence times and Leaf NPP_L . Notice that Hurricane Wilma impact data (2006) were excluded in these models (see discussion section).

anomalies at this site are attributed to natural variation in AGB likely caused by natural or lightning induced mortality (Whelan, 2005). Conversely, at SRS-6 the AGB anomalies increased negatively with time after Wilma (Fig. 3b), illustrating the influence of Wilma-induced mortality and the delayed mortality effect registered over a period of 6 years after disturbance. At SRS-4, the anomalies increased positively with time, underscoring the observed density variability and resulting increase in BA total value. The anomaly magnitude and range highlight the spatial variability in forest structure resistance to Wilma.

The complexity index (CI) calculated for each forest summarizes and integrates structural components in a single value. Early studies showed that this multiplicative index can quantitatively compare mangrove ecotypes (i.e., scrub, fringe, basin) characterized by a particular forest structure (Pool et al., 1977; Lugo, 1980). We used the CI to compare sites of the same ecotype (riverine), but with different abiotic environmental conditions (e.g., soil total phosphorus and salinity; Chen and Twilley, 1998; Rivera-Monroy et al., 2011; Castañeda-Moya et al., 2013). Riverine mangroves had pre-Wilma CI values ranging from 15 to 47 (Fig. 4); this range highlights the significant differences in height, BA, and density. The initial CI values at the study sites were comparable to other values reported for neotropical fringe and riverine mangrove forests (range: 4.9-97.5; Pool et al., 1977; Chen and Twilley, 1998; Castañeda-Moya et al., 2006). Temporal changes in CI were only evident at the SRS-6 site and indicate the significant decline in BA and tree density after storm impact (Fig. 4).

Evaluating the forest CI before a major disturbance is a useful baseline for determining Wilma's relative impact on forest complexity. For instance, Hurricane Joan (1988) significantly diminished the CI (from 4.3 to 0.6) in a riverine mangrove forest in Nicaragua (Roth, 1992). A category 4 hurricane at landfall, Hurricane Joan caused 36% stem mortality and induced a significant decrease (95%) in CI;

comparatively, Wilma caused 15% mortality, yet no significant decline in forest structure (36% decrease in CI). This comparison between disturbance magnitudes suggests that a threshold for structural resistance may lie between 15% and 36% stem mortality. For instance, Hurricane Mitch (1998, category 4) caused nearly 100% defoliation and 97% mortality, in a basin forest in Guanaja, Honduras and initial recovery assessments (15 months after impact) showed no evidence of colonization (Cahoon et al., 2003). The lack of seedling presence, and the resulting peat collapse due to stem mortality indicated that the forest was unlikely to recover, although subsequent data are not available to evaluate recovery (Smith et al., 2009). Hence, total mortality from hurricane disturbance does not necessarily define the resilience threshold since recovery from a major disturbance is a long process depending not only on the storm intensity, but also cumulative impacts regulated by both regional eco-geomorphology and climate change (Peterson et al., 1998; Fromard et al., 2004; Isbell et al., 2015; Duveneck and Scheller, 2016).

4.2. Functional properties

Following massive canopy defoliation, trees are expected to allocate more energy to foliage production for expedited refoliation (Craighead and Gilbert, 1962; Tanner et al., 1991; Stanturf et al., 2007; Jentsch et al., 2011), thus potentially arresting stem growth (DBH and height) and development (Bongers and Popma, 1990; Hikosaka, 2005). We did not find this pattern following Wilma; NPP_S was not arrested during NPP_L recovery (Danielson et al., 2017). Further, NPP_S did not differ between pre- and immediate-post Wilma (Fig. 5), indicating that NPP_S was resistant to the level of disturbance caused by the storm.

Forest canopy recovery after defoliation caused by storms depends on the initial intensity of the disturbance and pre-storm plant speciesspecific leaf turnover rates (Frolking et al., 2009). Since both leaf turnover and residence time are key processes leading to maximization of carbon gain and resource-use efficiency, it is critical to evaluate how these processes change as the forest return to a pre-disturbance state (Hikosaka, 2005). We estimated foliar residence time as a proxy to determine how fast canopy biomass was reestablished in response to the varying levels of defoliation caused by Wilma. Foliar residence time is defined in this study as the number of years the canopy foliage stays in the canopy compartment based on the leaf stock (i.e., leaf biomass) and leaf NPP_L flux (Danielson et al., 2017) (Fig. 6a). Leaf life span (i.e., residence times) is associated with leaf productivity rates, leaf physiology (i.e., nutrient translocation) and ecosystem processes (i.e., nutrient availability, litter turnover) (Chapin, 1980; Ellison, 2002; Hikosaka, 2005). For example, in south Florida, scrub mangroves have lower productivity due to hydrological and fertility stress conditions compared to riverine mangroves and therefore have greater longevity of leaves and roots (Castañeda-Moya et al., 2010; Castañeda-Moya et al., 2011; Castañeda-Moya et al., 2013). We found an inverse spatial relationship between leaf productivity and foliar residence time: residence time significantly increased with distance inland from the mouth of the estuary, with higher values upstream (SRS-4, $0.85 \pm 0.1 \,\mathrm{yr}$). This pattern supports the observed canopy NPP_L trend where the highest rates are observed in SRS-6 (Danielson et al., 2017). Residence time of the immediate-post-Wilma period was significantly different from pre- and post-Wilma periods as a result of the immediate decline in litterfall in 2006 due to defoliation (Danielson et al 2017). As NPP_L recovered, leaf residence time rates decreased returning to initial pre-Wilma values. Hence, leaf canopy residence time can be used as a good proxy for assessing forest resilience.

To further measure recovery trajectories, we determined the relationship of foliar residence time to annual leaf biomass anomalies (mean AGB % change from 2000 to 2001) and leaf NPP $_{\rm L}$ data. There was a positive relationship between leaf biomass anomalies (Fig. 3b) and foliar residence time across sites, where negative anomalies, which indicate a reduction in leaf biomass, caused shorter foliar residence

times (Fig. 6b). For instance, in SRS-6 residence time was 0.24 yr when there was a -28% anomaly in 2013. While leaf NPP_L had recovered at this site by 2013 (see Danielson et al., 2017), the leaf biomass stock has been reduced and had not recovered to pre-Wilma levels. Thus, the spatial variability in residence time and leaf AGB anomalies is a function of Wilma impact (i.e., mortality and defoliation) and recovery time for each site (Fig. 6b).

Leaf NPP_L vs foliar residence time showed a negative linear relationship ($R^2 = 0.88$; P < 0.001), where an increase in litterfall production resulted in a shorter residence time (Fig. 7a) and corresponded to different NPP_L storm recovery periods across sites. To determine the site-specific linear regression between foliar residence times and leaf NPP₁ before and after storm impact, we excluded the year 2006 (i.e. immediate after Wilma impact) when residence values were the highest and leaf NPPL was the lowest (Fig. 7b). The slope in this linear relationship was higher (-0.176) in SRS-4 since NPP_L has still not recovered (Danielson et al., 2017) (Fig. 7b), and therefore there was a wide range in residence time values (0.6-1.7 yr) indicating major differences in inter-annual NPP_L variation. At SRS-5, there was also a significant linear relationship, but the slope was lower (-0.076); NPP_L recovered after four years and showed a greater inter-annual variability $(5.4-7.4 \text{ Mg C ha}^{-1} \text{ yr}^{-1})$ when compared to SRS-4 (Fig. 7b). In SRS-6, NPP_L recovered to initial values at a faster rate (Danielson et al 2017) within a small range group (7.9–8.5, N = 6) in NPP_L values (7.9–8.5 Mg C $ha^{-1} yr^{-1}$), and as a result, a non-significant relationship with residence time ($R^2 = 0.30$; P = 0.20) (Fig. 7b). Thus, the NPP_L recovery trajectory observed at each site could be represented by the magnitude of the linear model slope, which integrates the interaction among site fertility, forest structure, and degree of disturbance impact. Since the relationship implicitly includes time (i.e., interannual NPP_L variability), we propose that the model slope could be used as proxy of canopy recovery in comparative studies with other mangrove ecotypes in different latitudes and geomorphic settings.

Comparing NPP_L to mortality and AGB shows a distinct trend of their relationship in the long term after a major disturbance (Fig. 8). Most notably in SRS-6, where canopy defoliation was the highest, wood AGB had a delayed response to Wilma, while NPP_L had an immediate response, and a four-year recovery period. Despite the long-term decline in AGB in SRS-6, a fast recovery in NPP_L was observed (i.e., inverse relationship; Fig. 7a). This indicates that even after a major decline in CI value, the forest stand in this site was able to recover, probably due to the deposition of inorganic phosphorus increasing site fertility (Castañeda-Moya et al., 2010) (see below). This inverse relationship also suggests a threshold of the total AGB needed to maintain a critical ecosystem function such as NPP_L.

4.3. Response trajectory

Forest gap and patch dynamic studies show that processes filling an impacted forest matrix space by natural disturbances of different scale are complex and interconnected in a number of forest ecosystems (McCarthy, 2001). Both gaps and patches significantly regulate abiotic conditions (e.g., light availability, evapotranspiration rates) which control in situ biotic processes (e.g., seedling growth, nutrient availability) (Shiels et al., 2015). Although gap dynamics has been evaluated in mangrove forests (e.g., Duke, 2001; Vogt et al., 2014), patch dynamics and its interaction with processes controlling gap formation and extension has been more limited (Smith et al., 2009; Rivera-Monrov et al., 2011). In the Everglades, lightning strikes create distinct gaps in the forest canopy affecting mangrove forests structure, and depending on the intensity, stem mortality and defoliation (Smith et al., 1994; Doyle et al., 1995; Smith et al., 2009; Rivera-Monroy et al., 2011; Barr et al., 2012). In the Everglades, the gap area is estimated to be about 4-5% of the total forest area with an average annual gap formation rate of approximately 0.3% of the total forest area per year (Zhang, 2008). Further, gap size across the southwestern region follows an exponential form where the area of gaps with sizes > 100 m² accounted for 55-61% of the total gap area (Zhang, 2008). Gaps originally created by lighting can be recognized after hurricane impacts when smaller gaps with vegetation in early stages of growth and development (tree height < 5 m) remain intact, while the surrounding forest matrix shifts to extensive open patch areas where the canopy was removed as result of tree fall/mortality (Zhang et al., 2008) or massive defoliation (Danielson et al., 2017). For instance, in 2005 numerous canopy gaps and patches were created after Wilma; from ~400-500 to 4,000 per km² (Zhang, 2008). Yet, despite this information, no functional landscape connection has been quantitative established once gaps $(\leq 200 \,\mathrm{m}^2)$ expand into patches (> 200 m²) (McCarthy, 2001) as result of hurricane impact.

Our long-term demography study pre- and post- Wilma impact show that gap and patch dynamics and mangrove succession are inextricably linked, yet this interaction is not well understood (Rivera-Monroy et al., 2011). It is estimated that the relative contribution of hurricanes to mangrove forest disturbance in the Everglades is at least 2x more than that from lightning strikes (Zhang et al., 2008). Therefore, this differential contribution in canopy opening dimensions creates complex heterogeneous mosaic of gap/patches of different age where successional stages are non-linear and in non-steady state as observed in other mangrove forests impacted by tropical storms (Ball, 1980; Alongi, 2008; Lugo, 2008; Vogt et al., 2014; Imbert, 2018). While lightning strikes usually do not change the community structure of the forest

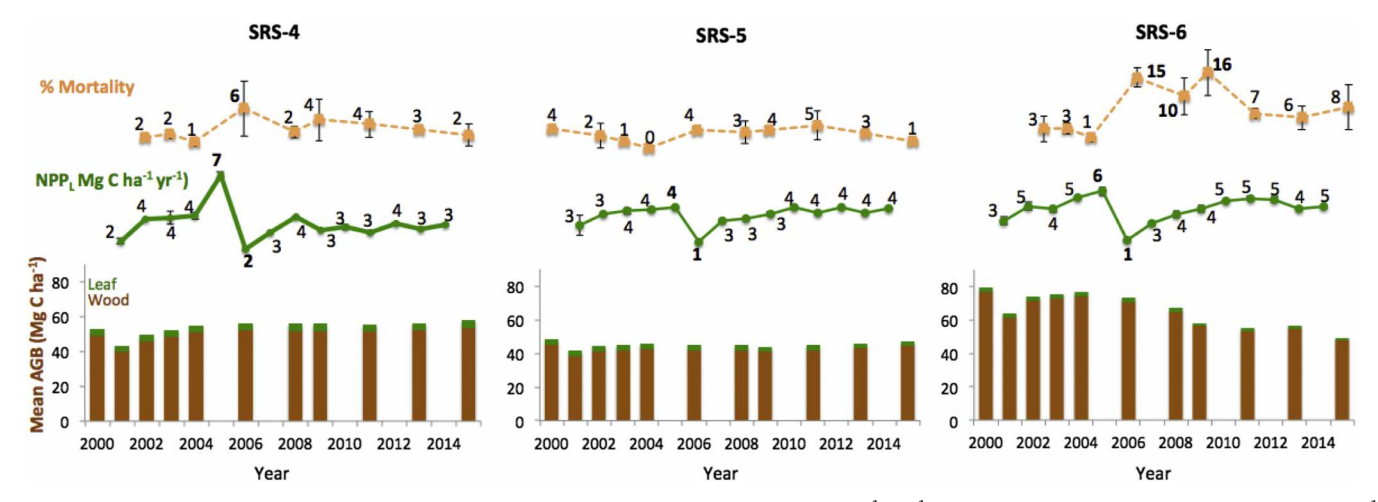


Fig. 8. Composite of percent (%) mortality, mean net litterfall primary productivity (NPP_L, Mg C ha^{-1} yr⁻¹), and mean aboveground biomass (AGB, Mg C ha^{-1}) variables per site from 2000 to 2015

surrounding a gap (Whelan, 2005), hurricane impacts can produce dramatic changes in the surrounding forest matrix (e.g., expanding/ merging gaps into patch dimension), which in turn may feedback on processes within the gap itself (Rivera-Monroy et al., 2011). For instance, Wilma's extensive defoliation across sites lead to variations in long-term dynamics by increasing light availability to the understory as observed in SRS-5 (Fig. 2). In this site, L. racemosa BA increased as saplings grew and progressed into new recruits (DBH > 2.5 cm), as indicated by the recruitment of individuals into the 2.5 size class in the post-Wilma period (Fig. 2). Similarly, the stem productivity increased by 62% immediate-post-Wilma, especially in the case of the L. racemosa species (Fig. 5). Generally, gaps in SRS-5 are eventually filled by the species R. mangle (a shade tolerant species: Ball, 1980; Chen and Twilley, 1998; Whelan, 2005), which is the dominant species in this site (Fig. S3) (Chen and Twilley, 1999; Castañeda-Moya et al., 2013). Comparatively, in the SRS-6 site where L. racemosa is the dominant species, NPPs decreased by 22% in the post-Wilma period due to extensive defoliation and tree mortality (Figs. S2, 8), yet species composition and size distribution were not significantly modified (Fig. S3). We attribute this outcome to the ecophysiological response of L. racemosa to extensive light availability since this species is considered shade intolerant (Ball, 1980; Ross et al., 2006; Lopez-Hoffman et al., 2007). It seems that the gap size in SRS-5 (mean: $202 \pm 16 \,\mathrm{m}^2$; Whelan 2005) influence the amount of light (i.e., Photosynthetic Active Radiation -PAR) reaching the gap/patch forest floor throughout the year. We hypothesize that the persistent dominance of the L racemosa species in SRS-6 is due to the impact of hurricanes promoting extensive light availability due to the formation of large patches, particularly close to the Shark River estuary mouth (Chen and Twilley, 1998).

In addition to light availability, the recovery trajectory is also influenced by hurricane storm surge, which alters soil elevation and nutrient dynamics (Cahoon et al., 2003; Whelan et al., 2009; Castañeda-Moya et al., 2010). Nutrient inputs from hurricanes also lead to positive recovery responses, especially in forests that are nutrient limited like the Everglades (Lugo, 1980; Feller et al., 2003; Feller et al., 2015). In this region, Wilma storm surge decreased from 3 to 4 m at SRS-6 to 0.5 m at SRS-4 (Castañeda-Moya et al., 2010) (Fig. 1). This surge deposited mineral sediments (0.5–2.5 cm) with significantly higher total phosphorus (TP) concentrations (0.36 mg cm⁻³) than in the surface (top 10 cm) soil layer (0.22 mg cm⁻³) (Castañeda-Moya et al., 2010). We propose that this TP storm deposition supported tree nutrient demand for both stem and litterfall productivity during refoliation after storm impact (i.e., a positive feedback), particularly at SRS-6, thus contributing to a faster forest recovery (Danielson et al., 2017).

Soil pore water salinity, a major regulator of mangrove structure and productivity (Twilley and Rivera-Monroy, 2009), can also limit both leaf and stem NPP if concentrations are high (> 70 ppt) (e.g., Castañeda-Moya et al., 2006). Conversely, low salinity (< 5 ppt) reduces the competitive advantage of mangroves over freshwater vegetation (Kristensen et al., 2017). Current and previous studies show that the SRS-4 site is becoming fresher (< 5 ppt), as indicated by long-term soil pore-water measurements (Rivera-Monroy, unpublished data). Although AGB was unaffected at SRS-4, NPPs declined by 30% in the post-Wilma period (Fig. 5). We further propose that the intraspecific competition for resources (e.g., light, nutrients) with dominant vegetation in freshwater /brackish environments (e.g., cocoplum, *Chrysobalamus icaco*; golden leather fern, *Acrostichum aureum*), which is present and expanding in SRS-4, have contributed to the long-term decline in mangrove wetland NPPs in this site.

4.4. Conclusions

We conclude that the SRS mangroves were resistant to Hurricane Wilma (2005) since mortality and defoliation did not cause significant changes to forest structure or stem productivity after impact (~ 10 years). Because mangrove wetlands in south Florida are

frequently subject to hurricanes, any increase in hurricane frequency and intensification will significantly impact forest dynamics. We discovered that the interaction between disturbance magnitude and sitespecific attributes (i.e., TP soil fertility, hydroperiod, species composition) resulted in differential changes in basal area, AGB and stem density values in the long-term. Our quantitative assessment of the mangrove forest response trajectory offers a baseline for disturbance modeling scenarios. Each site serves as a reference response for a particular disturbance magnitude that falls between the extremes of no impact (resistant) to no recovery (not resilient). These findings help define the mangrove resilience threshold by narrowing the spatiotemporal boundaries and defining the impact from a specific disturbance magnitude (Rever et al., 2015). Identifying the disturbance magnitude that will push the ecosystem past a threshold (i.e., tipping point) is critical to assess habitat shifts as result of the interaction between natural and anthropogenic disturbances (Gabler et al., 2017). This is especially important in the case of neotropical mangrove wetlands in northern latitudes, where large-scale disturbance is frequent, and greater intensity hurricanes are predicted to become the new normal (Webster et al., 2005; Osland et al., 2013; Tanner et al., 2014; Murakami et al., 2018; Simard et al., 2019). For example, mangrove demographic models developed for neotropical mangroves (Berger et al., 2008), such as the FORMAN and KiWi, will particularly benefit from this spatially relevant, quantitative data and information to facilitate the calibration and validation of these models under different scenarios of climate variability and change (Piou et al., 2008; Vogt et al., 2012; Vogt et al., 2014).

Determining how large-scale disturbance events impact carbon budgets is a major research gap in wetlands in general (e.g., Engle, 2011; Villa and Bernal, 2018), and mangrove forests in particular, given their significant carbon storage and sequestration rates (Rivera-Monroy et al., 2013; Rovai et al., 2016; Sanderman et al., 2018; Twilley et al., 2018; Simard et al., 2019). For instance, it is estimated that Everglades mangrove wetlands currently store total organic carbon (above and belowground) in the range of 70 to 537 Mg C/ha (Jerath et al., 2016). This allocation of organic carbon into forest components is an ecosystem service with an estimated economic value ranging from \$2-3.4 billion dollars and highlights the priority in assessing hurricane impacts on AGB in the long term (Jerath et al., 2016). One major conclusion in our study is that given the storm magnitude (category 3) and trajectory, carbon stocks (i.e., AGB) along Shark River were not significantly reduced or lost. Our work assessed for the first time in northern neotropical latitudes the long-term response of mangrove forest carbon stocks to a major landscape level-disturbance. Although Wilma was not a highly destructive storm, its impact allowed the determination of the magnitude, direction, and time span within which mangroves respond to a wide range of structural damage. These findings contribute to advancing ecological disturbance theory and modeling of forested wetland by providing quantitative relationships among dynamic processes to validate demographic and mechanistic mangrove model needed in Earth system models (Claussen et al., 2002).

Acknowledgements

This project was funded by the National Science Foundation (NSF) through the Florida Coastal Everglades Long-Term Ecological Research (FCE LTER) program under cooperative agreements #DBI-0620409, and #DEB-9910514. The NASA-JPL project 'Vulnerability Assessment of Mangrove Forest Regions of the Americas' (LSU Subcontract no. 1452878) and the Department of the Interior South-Central Climate Adaptation Science Center (Cooperative Agreement #G12AC00002) provided partial funding to VHRM. We thank Robert R. Twilley and Daniel Childers for designing and implementing mangrove research initiatives in the FCE (2001-2005) that currently support this type of studies. Special thanks to the Everglades National Park for granting research permits and the Florida Bay Interagency Science Center-

Everglades National Park (FBISC-ENP) for logistic support during the study. We also acknowledge Narinder Heer (LSU) for statistical analyses assistance. We are grateful for the field support provided by Meenakshi Jareth, Luca Marazzi, Imani Maxberry and a number of LSU and FIU undergraduate and graduate students through the study. This paper is based on a master thesis submitted to the Department of Oceanography and Coastal Sciences, Louisiana State University by TMD.

Appendix A. Supplementary material

Supplementary data to this article can be found online at https://doi.org/10.1016/j.foreco.2019.02.036.

References

- Alongi, D.M., 2008. Mangrove forests: Resilience, protection from tsunamis, and responses to global climate change. Estuar. Coast. Shelf Sci. 76, 1–13.
- Angeler, D.G., Allen, C.R., 2016. Quantifying resilience. J. Appl. Ecol. 53, 617–624.Baldwin, A.H., Platt, W.J., Gathen, K.L., Lessmann, J.M., Rauch, T.J., 1995. Hurricane damage and regeneration in fringe Mangrove forests of Southeast Florida, USA. J. Coastal Res. 21, 169–183.
- Baldwin, A., Egnotovich, M., Ford, M., Platt, W., 2001. Regeneration in fringe mangrove forests damaged by Hurricane Andrew. Plant Ecol. 157, 151–164.
- Ball, M.C., 1980. Patterns off secondary succession in a mangrove forest of Southern Florida. 44, 226–235.
- Barr, J.G., Engel, V., Smith, T.J., Fuentes, J.D., 2012. Hurricane disturbance and recovery of energy balance, CO₂ fluxes and canopy structure in a mangrove forest of the Florida Everglades. Agric. For. Meteorol. 153, 54–66.
- Becknell, J.M., Desai, A.R., Dietze, M.C., Schultz, C.A., Starr, G., Duffy, P.A., Franklin, J.F., Pourmokhtarian, A., Hall, J., Stoy, P.C., Binford, M.W., Boring, L.R., Staudhammer, C.L., 2015. Assessing interactions among changing climate, management, and disturbance in forests: a macrosystems approach. Bioscience 65, 263–274.
- Berger, U., Rivera-Monroy, V.H., Doyle, T.W., Dahdouh-Guebas, F., Duke, N.C., Fontalvo-Herazo, M.L., Hildenbrandt, H., Koedam, N., Mehlig, U., Piou, C., Twilley, R.R., 2008. Advances and limitations of individual-based models to analyze and predict dynamics of mangrove forests: A review. Aquat. Bot. 89, 260–274.
- Bernhardt, J.R., Leslie, H.M., 2013. Resilience to climate change in coastal marine ecosystems. In: Carlson, C.A., Giovannoni, S.J. (Eds.). Annual Review of Marine Science, vol. 5, pp. 371–392.
- Beven, J.L., Avila, L.A., Blake, E.S., Brown, D.P., Franklin, J.L., Knabb, R.D., Pasch, R.J., Rhome, J.R., Stewart, S.R., 2008. Atlantic hurricane season of 2005. Mon. Weather Rev. 136, 1109–1173.
- Bhatia, K., Vecchi, G., Murakami, H., Underwood, S., Kossin, J., 2018. Projected response of tropical cyclone intensity and intensification in a global climate model. J. Clim. 31, 8281–8303
- Bhatia, K.T., Vecchi, G.A., Knutson, T.R., Murakami, H., Kossin, J., Dixon, K.W., Whitlock, C.E., 2019. Recent increases in tropical cyclone intensification rates. Nat. Commun. 10 1–9
- Bongers, F., Popma, J., 1990. Leaf dynamcis of seedlings of rain-forest species in relation to canopy gaps. Oecologia 82, 122–127.
- Busing, R.T., Mailly, D., 2004. Advances in spatial, individual-based modelling of forest dynamics. J. Veg. Sci. 15, 831–842.
- Busing, R.T., White, R.D., Harmon, M.E., White, P.S., 2009. Hurricane disturbance in a temperate deciduous forest: patch dynamics, tree mortality, and coarse woody detritus. Plant Ecol. 201, 351–363.
- Cahoon, D.R., Hensel, P., Rybczyk, J., McKee, K.L., Proffitt, C.E., Perez, B.C., 2003. Mass tree mortality leads to mangrove peat collapse at Bay Islands, Honduras after Hurricane Mitch. J. Ecol. 91, 1093–1105.
- Castañeda-Moya, E., Rivera-Monroy, V.H., Twilley, R.R., 2006. Mangrove zonation in the dry life zone of the Gulf of Fonseca, Honduras. Estuaries Coasts 29, 751–764.
- Castañeda-Moya, E., Twilley, R.R., Rivera-Monroy, V.H., 2013. Allocation of biomass and net primary productivity of mangrove forests along environmental gradients in the Florida Coastal Everglades, USA. For. Ecol. Manage. 307, 226–241.
- Castañeda-Moya, E., Twilley, R.R., Rivera-Monroy, V.H., Marx, B.D., Coronado-Molina, C., Ewe, S.M.L., 2011. Patterns of root dynamics in mangrove forests along environmental gradients in the florida coastal everglades, USA. Ecosystems 14, 1178–1195.
- Castañeda-Moya, E., Twilley, R.R., Rivera-Monroy, V.H., Zhang, K.Q., Davis, S.E., Ross, M., 2010. Sediment and nutrient deposition associated with hurricane wilma in mangroves of the florida coastal everglades. Estuaries Coasts 33, 45–58.
- Chao, Y.Y., Tolman, H.L., 2010. Performance of NCEP regional wave models in predicting peak sea states during the 2005 north atlantic hurricane season. Weather Forecasting 25, 1543–1567.
- Chapin, F.S., 1980. The mineral nutrition of wild plants. Annu. Rev. Ecol. Syst. 11, 233–260.
- Chen, R., Twilley, R.R., 1998. A gap dynamic model of mangrove forest development along gradients of soil salinity and nutrient resources. J. Ecol. 86, 1–12.
- Chen, R.H., Twilley, R.R., 1999. Patterns of mangrove forest structure and soil nutrient dynamics along the Shark River estuary, Florida. Estuaries 22, 955–970.
- Claussen, M., Mysak, L.A., Weaver, A.J., Crucifix, M., Fichefet, T., Loutre, M.F., Weber, S.L., Alcamo, J., Alexeev, V.A., Berger, A., Calov, R., Ganopolski, A., Goosse, H.,

- Lohmann, G., Lunkeit, F., Mokhov, I.I., Petoukhov, V., Stone, P., Wang, Z., 2002. Earth system models of intermediate complexity: closing the gap in the spectrum of climate system models. Clim. Dynam. 18, 579–586.
- Collins, S.L., Carpenter, S.R., Swinton, S.M., Orenstein, D.E., Childers, D.L., Gragson, T.L., Grimm, N.B., Grove, M., Harlan, S.L., Kaye, J.P., Knapp, A.K., Kofinas, G.P., Magnuson, J.J., McDowell, W.H., Melack, J.M., Ogden, L.A., Robertson, G.P., Smith, M.D., Whitmer, A.C., 2011. An integrated conceptual framework for long-term social-ecological research. Front. Ecol. Environ. 9, 351–357.
- Costa, P., Dorea, A., Mariano-Neto, E., Barros, F., 2015. Are there general spatial patterns of mangrove structure and composition along estuarine salinity gradients in Todos os Santos Bay? Estuar. Coast. Shelf Sci. 166, 83–91.
- Craighead, F.C., Gilbert, V.C., 1962. The effects of hurricane donna on the vegetation of southern Florida. Quart. J. Florida Acad. Sci. 25, 1–28.
- Danielson, T.M., Rivera-Monroy, V.H., Castaneda-Moya, E., Briceno, H., Travieso, R., Marx, B.D., Gaiser, E., Farfan, L.M., 2017. Assessment of Everglades mangrove forest resilience: Implications for above-ground net primary productivity and carbon dynamics. For. Ecol. Manage. 404, 115–125.
- Doyle, T.W., Krauss, K.W., Wells, C.J., 2009. Landscape analysis and patterns of Hurricane impact and circulation on mangrove forests of the Everglades. Wetlands 29, 44–53.
- Doyle, T.W., Smith, T.J., Robblee, M.B., 1995. Wind damage effects of Hurricane Andrew on mangrove communities along the southwest coast of Florida, USA. J. Coastal Res. 81, 159–168.
- Duke, N.C., 2001. Gap creation and regenerative process driving diversity and structure of mangrove ecosystems. Wetlands Ecol. Manage. 9, 257–269.
- Duveneck, M.J., Scheller, R.M., 2016. Measuring and managing resistance and resilience under climate change in northern Great Lake forests (USA). Landscape Ecol. 31, 669–686.
- Ellison, A.M., 2002. Macroecology of mangroves: large-scale patterns and processes in tropical coastal forests. Trees-Struct. Funct. 16, 181–194.
- Engle, V.D., 2011. Estimating the provision of ecosystem services by gulf of Mexico coastal wetlands. Wetlands 31, 179–193.
- Farfan, L.M., D'Sa, E.J., Liu, K.-B., Rivera-Monroy, V.H., 2014. Tropical cyclone impacts on coastal regions: the case of the Yucatan and the Baja California Peninsulas, Mexico. Estuaries Coasts 37, 1388–1402.
- Feller, I.C., Dangremond, E.M., Devlin, D.J., Lovelock, C.E., Proffitt, C.E., Rodriguez, W., 2015. Nutrient enrichment intensifies hurricane impact in scrub mangrove ecosystems in the Indian River Lagoon, Florida, USA. Ecology 96, 2960–2972.
- Feller, I.C., Whigham, D.F., McKee, K.L., Lovelock, C.E., 2003. Nitrogen limitation of growth and nutrient dynamics in a disturbed mangrove forest, Indian River Lagoon, Florida. Oecologia 134, 405–414.
- Frolking, S., Palace, M.W., Clark, D.B., Chambers, J.Q., Shugart, H.H., Hurtt, G.C., 2009. Forest disturbance and recovery: A general review in the context of spaceborne remote sensing of impacts on aboveground biomass and canopy structure. J. Geophys. Res.-Biogeo. 114.
- Fromard, F., Vega, C., Proisy, C., 2004. Half a century of dynamic coastal change affecting mangrove shorelines of French Guiana. A case study based on remote sensing data analyses and field surveys. Mar. Geol. 208, 265–280.
- Gabler, C.A., Osland, M.J., Grace, J.B., Stagg, C.L., Day, R.H., Hartley, S.B., Enwright, N.M., From, A.S., McCoy, M.L., McLeod, J.L., 2017. Macroclimatic change expected to transform coastal wetland ecosystems this century. Nature. Clim. Change 7, 142.+
- Gilman, E.L., Ellison, J., Duke, N.C., Field, C., 2008. Threats to mangroves from climate change and adaptation options: A review. Aquat. Bot. 89, 237–250.
- Hikosaka, K., 2005. Leaf canopy as a dynamic system: Ecophysiology and optimality in leaf turnover. Ann. Bot.-Lond. 95, 521-533.
- Holdridge, L.R., Grenke, W.C., Hatheway, W.H., Liang, T., Tosi, J.A., 1971. Forest environments in tropical life zones: a pilot study. Pergamom Press Inc, New York.
- Host, G.E., Stech, H.W., Lenz, K.E., Roskoski, K., Mather, R., 2008. Forest patch modeling: using high performance computing to simulate aboveground interactions among individual trees. Funct. Plant Biol. 35, 976–987.
- Imbert, D., 2018. Hurricane disturbance and forest dynamics in east Caribbean mangroves. Ecosphere 9, 13.
- Isbell, F., Craven, D., Connolly, J., Loreau, M., Schmid, B., Beierkuhnlein, C., Bezemer, T.M., Bonin, C., Bruelheide, H., de Luca, E., Ebeling, A., Griffin, J.N., Guo, Q.F., Hautier, Y., Hector, A., Jentsch, A., Kreyling, J., Lanta, V., Manning, P., Meyer, S.T., Mori, A.S., Naeem, S., Niklaus, P.A., Polley, H.W., Reich, P.B., Roscher, C., Seabloom, E.W., Smith, M.D., Thakur, M.P., Tilman, D., Tracy, B.F., van der Putten, W.H., van Ruijven, J., Weigelt, A., Weisser, W.W., Wilsey, B., Eisenhauer, N., 2015. Biodiversity increases the resistance of ecosystem productivity to climate extremes. Nature 526, 574–U263.
- Jentsch, A., Kreyling, J., Elmer, M., Gellesch, E., Glaser, B., Grant, K., Hein, R., Lara, M., Mirzae, H., Nadler, S.E., Nagy, L., Otieno, D., Pritsch, K., Rascher, U., Schadler, M., Schloter, M., Singh, B.K., Stadler, J., Walter, J., Wellstein, C., Wollecke, J., Beierkuhnlein, C., 2011. Climate extremes initiate ecosystem-regulating functions while maintaining productivity. J. Ecol. 99, 689–702.
- Jerath, M., Bhat, M., Rivera-Monroy, V.H., Castaneda-Moya, E., Simard, M., Twilley, R.R., 2016. The role of economic, policy, and ecological factors in estimating the value of carbon stocks in Everglades mangrove forests, South Florida, USA. Environ. Sci. Policy 66, 160–169.
- Knutson, T.R., McBride, J.L., Chan, J., Emanuel, K., Holland, G., Landsea, C., Held, I., Kossin, J.P., Srivastava, A.K., Sugi, M., 2010. Tropical cyclones and climate change. Nat. Geosci. 3, 157.
- Kristensen, E., Connolly, R.M., Otero, X.L., Marchand, M., Ferreira, T.O., Rivera-Monroy, V.H., 2017. Chapter 11. Biogeochemical cycles: Global approaches and perspectives. In: Rivera-Monroy, V.H., Lee, S.Y., Kristensen, E., Twilley, R.R. (Eds.), Mangrove

- Ecosystems: A Global Biogeographic Perspective Structure, Function and Ecosystem Services. Springer, New York, pp. 163–209.
- Lacambra, C., Friess, T.S., Möller, I., 2013. Bioshields: Mangrove ecosystems as resilient natural coastal defenses. In: Renaud, F.G., Sudmeier-Rieux, K., Estrella, M. (Eds.), The role of ecosystems in disaster risk reduction. UNU Press, Tokyo.
- Lopez-Hoffman, L., Ackerly, D.D., Anten, N.P.R., Denoyer, J.L., Martinez-Ramos, M., 2007. Gap-dependence in mangrove life-history strategies: A consideration of the entire life cycle and patch dynamics. J. Ecol. 95, 1222–1233.
- Lucash, M.S., Scheller, R.M., Sturtevant, B.R., Gustafson, E.J., Kretchun, A.M., Foster, J.R., 2018. More than the sum of its parts: how disturbance interactions shape forest dynamics under climate change. Ecosphere 9.
- Lugo, A.E., 1980. Mangrove ecosystems: successional or steady state? Trop Succ 65–72.Lugo, A.E., 2008. Visible and invisible effects of hurricanes on forest ecosystems: an international review. Austral Ecol. 33, 368–398.
- Macamo, C.C.F., Massuanganhe, E., Nicolau, D.K., Bandeira, S.O., Adams, J.B., 2016.
 Mangrove's response to cyclone Eline (2000): What is happening 14 years later.
 Aquat. Bot. 134, 10–17.
- McCarthy, J., 2001. Gap dynamics of forest trees: A review with particular attention to boreal forests. Environ. Rev. 9, 1–59.
- McCarthy, J.W., Weetman, G., 2006. Age and size structure of gap-dynamic, old-growth boreal forest stands in Newfoundland. Silva. Fenn. 40, 209–230.
- Milbrandt, E.C., Greenawalt-Boswell, J.M., Sokoloff, P.D., Bortone, S.A., 2006. Impact and response of southwest Florida mangroves to the 2004 hurricane season. Estuaries Coasts 29, 979–984.
- Murakami, A.A., Levin, E., Delworth, T.L., Gudgel, R., Hsu, P.-C., 2018. Dominant effect of relative tropiacl Atlantic warming on major hurricane occurrence. Science 362, 794–799.
- Nehru, P., Balasubramanian, P., 2018. Mangrove species diversity and composition in the successional habitats of Nicobar Islands, India: A post-tsunami and subsidence scenario. For. Ecol. Manage. 427, 70–77.
- Osland, M.J., Day, R.H., Hall, C.T., Brumfield, M.D., Dugas, J.L., Jones, W.R., 2017.

 Mangrove expansion and contraction at a poleward range limit: climate extremes and land-ocean temperature gradients. Ecology 98, 125–137.
- Osland, M.J., Enwright, N., Day, R.H., Doyle, T.W., 2013. Winter climate change and coastal wetland foundation species: salt marshes vs. mangrove forests in the southeastern United States. Glob. Change Biol. 19, 1482–1494.
- Osland, M.J., Feher, L.C., Lopez-Portillo, J., Day, H.R., Suman, D.O., Guzman-Menendez, J.M., Rvera-Monroy, V.H., 2018. Mangrove forests in a rapidly changing world: global change impacts and conservation opportunities along the Gulf of Mexico coast. Estuarine Coastal Shelf Sci. 214, 120–140.
- Peterson, G., Allen, C.R., Holling, C.S., 1998. Ecological resilience, biodiversity, and scale. Ecosystems 1, 6–18.
- Pickett, S.T.A., Kolasa, J., Armesto, J.J., Collins, S.L., 1989. The ecological concept of disturbance and its expression at various hierarchical levels. Oikos 54, 129–136.
- Piou, C., Berger, U., Hildenbrandt, H., Feller, I.C., 2008. Testing the intermediate disturbance hypothesis in species-poor systems: A simulation experiment for mangrove forests. J. Veg. Sci. 19, 417–U153.
- Pool, D.J., Snedaker, S.C., Lugo, A.E., 1977. Structure of Mangrove Forests in Florida, Puerto Rico, Mexico, and Costa Rica. Biotropica 9, 195–212.
- Reyer, C.P.O., Brouwers, N., Rammig, A., Brook, B.W., Epila, J., Grant, R.F., Holmgren, M., Langerwisch, F., Leuzinger, S., Lucht, W., Medlyn, B., Pfeifer, M., Steinkamp, J., Vanderwel, M.C., Verbeeck, H., Villela, D.M., 2015. Forest resilience and tipping points at different spatio-temporal scales: approaches and challenges. J. Ecol. 103, 5–15.
- Rivera-Monroy, V.H., Castañeda-Moya, E., Barr, J.G., Engel, V., Fuentes, J.D., Troxler, T.G., Twilley, R.R., Bouillon, S., Smith, T.J., O'Halloran, T.L., 2013. Current methods to evaluate net primary production and carbon budgets in mangrove forests. In: DeLaune, R.D., Reddy, K.R., Megonigal, P., Richardson, C. (Eds.), Methods in Biogeochemistry of Wetlands. Soil Science Society of America Book Series, pp. 243–288
- Rivera-Monroy, V.H., Osland, M.J., Day, J.W., Ray, S., Rovai, A.S., Day, R.H., Mukherjee, J., 2017. Advancing Mangrove Macroecology. In: Rivera-Monroy, V.H., Kristensen, E., Lee, S.Y., Twilley, R.R. (Eds.), Mangrove Ecosystems: A Global Biogeographic Perspective: Structure, Function and Ecosystem Services. Springer, New York, pp. 347–371.
- Rivera-Monroy, V.H., Twilley, R.R., Davis, S.E., Childers, D.L., Simard, M., Chambers, R., Jaffe, R., Boyer, J.N., Rudnick, D.T., Zhang, K., Castaneda-Moya, E., Ewe, S.M.L., Price, R.M., Coronado-Molina, C., Ross, M., Smith, T.J., Michot, B., Meselhe, E., Nuttle, W., Troxler, T.G., Noe, G.B., 2011. The Role of the Everglades Mangrove Ecotone Region (EMER) in Regulating Nutrient Cycling and Wetland Productivity in South Florida. Critic. Rev. Environ. Sci. Technol. 41, 633–669.
- Romps, D.M., Seeley, J.T., Vollaro, D., Molinari, J., 2014. Projected increase in lightning strikes in the United States due to global warming. Science 346, 851–854.
- Ross, M.S., Ruiz, P.L., Sah, J.P., Reed, D.L., Walters, J., Meeder, J.F., 2006. Early post-hurricane stand development in Fringe mangrove forests of contrasting productivity. Plant Ecol. 185, 283–297.
- Roth, L.C., 1992. Hurricanes and mangrove regeneration: effects of Hurricane Joan, October 1988, on the Vegetation of Isla del Venado, Bluefields, Nicaragua. Biotropica 24, 375–384.
- Rovai, A.S., Riul, P., Twilley, R.R., Castaneda-Moya, E., Rivera-Monroy, V.H., Williams, A.A., Simard, M., Cifuentes-Jara, M., Lewis, R.R., Crooks, S., Horta, P.A., Schaeffer-

- Novelli, Y., Cintron, G., Pozo-Cajas, M., Pagliosa, P.R., 2016. Scaling mangrove aboveground biomass from site-level to continental-scale. Glob. Ecol. Biogeogr. 25, 286–298.
- Rovai, A.S., Twilley, R.R., Castaneda-Moya, E., Riul, P., Cifuentes-Jara, M., Manrow-Villalobos, M., Horta, P.A., Simonassi, J.C., Fonseca, A.L., Pagliosa, P.R., 2018. Global controls on carbon storage in mangrove soils. Nat. Clim. Change 8, 534–538.
- Saenger, P., Snedaker, S.C., 1993. Pantropical trends in mangroe aboveground biomass and annual litterfall. Oecologia 96, 293–299.
- Sanderman, J., Hengl, T., Fiske, G., Solvik, K., Adame, M.F., Benson, L., Bukoski, J.J., Carnell, P., Cifuentes-Jara, M., Donato, D., Duncan, C., Eid, E.M., zu Ermgassen, P., Lewis, C.J.E., Macreadie, P.I., Glass, L., Gress, S., Jardine, S.L., Jones, T.G., Nsombo, E.N., Rahman, M.M., Sanders, C.J., Spalding, M., Landis, E., 2018. A global map of mangrove forest soil carbon at 30 m spatial resolution. Environ. Res. Lett. 13.
- Seidl, R., Thom, D., Kautz, M., Martin-Benito, D., Peltoniemi, M., Vacchiano, G., Wild, J., Ascoli, D., Petr, M., Honkaniemi, J., Lexer, M.J., Trotsiuk, V., Mairota, P., Svoboda, M., Fabrika, M., Nagel, T.A., Reyer, C.P.O., 2017. Forest disturbances under climate change. Nat. Clim. Change 7, 395–402.
- Servino, R.N., Gomes, L.E.D., Bernardino, A.F., 2018. Extreme weather impacts on tropical mangrove forests in the Eastern Brazil Marine Ecoregion. Sci. Total Environ. 628–629, 233–240.
- Sherman, R.E., Fahey, T.J., Battles, J.J., 2000. Small-scale disturbance and regeneration dynamics in a neotropical mangrove forest. J. Ecol. 88, 165–178.
- Sherman, R.E., Fahey, T.J., Martinez, P., 2003. Spatial patterns of Biomass and above-ground net primary productivity in a mangrove ecosystem in the Dominican Republic. Ecosystems 6, 384–398.
- Shiels, A.B., Gonzalez, G., Lodge, D.J., Willig, M.R., Zimmerman, J.K., 2015. Cascading effects of canopy opening and debris deposition from a large-scale hurricane experiment in a tropical rain forest. Bioscience 65, 871–881.
- Simard, M., Fatoyinbo, L., Smetanka, C., Rivera-Monroy, V.H., Castaneda-Moya, E., Thomas, N., Van der Stocken, T., 2019. Mangrove canopy height globally related to precipitation, temperature and cyclone frequency. Nat. Geosci. 12, 40-+.
- Simard, M., Zhang, K.Q., Rivera-Monroy, V.H., Ross, M.S., Ruiz, P.L., Castaneda-Moya, E., Twilley, R.R., Rodriguez, E., 2006. Mapping height and biomass of mangrove forests in Everglades National Park with SRTM elevation data. Photogramm. Eng. Remote Sens. 72, 299–311.
- Sklar, F.H., Chimney, M.J., Newman, S., McCormick, P., Gawlik, D., Miao, S.L., McVoy, C., Said, W., Newman, J., Coronado, C., Crozier, G., Korvela, M., Rutchey, K., 2005. The ecological-societal underpinnings of Everglades restoration. Front. Ecol. Environ. 3, 161–169.
- Smith, T.J., Anderson, G.H., Balentine, K., Tiling, G., Ward, G.A., Whelan, K.R.T., 2009. Cumulative impacts of hurricanes on Florida mangrove ecosystems: sediment deposition, storm surges and vegetation. Wetlands 29, 24–34.
- Smith, T.J., Robblee, M.B., Wanless, H.R., Doyle, T.W., 1994. Mangroves, hurricanes, and lighting strikes. Bioscience 44, 256–262.
- Smith, T.J., Whelan, K.R.T., 2006. Development of allometric relations for three mangrove species in South Florida for use in the Greater Everglades Ecosystem restoration. Wetlands Ecol. Manage. 14, 409–419.
- Stanturf, J.A., Goodrick, S.L., Outcalt, K.W., 2007. Disturbance and coastal forests: A strategic approach to forest management in hurricane impact zones. For. Ecol. Manage. 250, 119–135.
- Sun, D.L., Lau, K.M., Kafatos, M., 2008. Contrasting the 2007 and 2005 hurricane seasons: Evidence of possible impacts of Saharan dry air and dust on tropical cyclone activity in the Atlantic basin. Geophys. Res. Lett. 35.
- Tanner, E.V.J., Kapos, V., Healey, J.R., 1991. Hurricane Effects on Forest Ecosystems in the Caribbean. Biotropica 23, 513–521.
- Tanner, E.V.J., Rodriguez-Sanchez, F., Healey, J.R., Holdaway, R.J., Bellingham, P.J., 2014. Long-term hurricane damage effects on tropical forest tree growth and mortality. Ecology 95, 2974–2983.
- Twilley, R., Rovai, A.S., Riul, P., 2018. Coastal morphology explains global blue carbon distributions. Front. Ecol. Environ. 16, 503–508.
- Twilley, R.R., Rivera-Monroy, V.H., 2009. Ecogeomorphic models of nutrient biogeochemistry for mangrove wetlands. In: Perillo, G.M., Wolanski, E., Cahoon, D.R., Brinson, M.M. (Eds.), Coastal Wetlands: An Integrated Ecosystem Approach. Elsevier, pp. 641–683.
- Twilley, R.R., Rivera-Monroy, V.H., Chen, R., Botero, L., 1998. Adapting and ecological mangrove model to simulate trajectories in restoration ecology. Mar. Pollut. Bull. 37, 404–419.
- Villa, J.A., Bernal, B., 2018. Carbon sequestration in wetlands, from science to practice: An overview of the biogeochemical process, measurement methods, and policy framework. Ecol. Eng. 114, 115–128.
- Vogt, J., Piou, C., Berger, U., 2014. Comparing the influence of large- and small-scale disturbances on forest heterogeneity: A simulation study for mangroves. Ecol. Complexity 20, 107–115.
- Vogt, J., Skora, A., Feller, I.C., Piou, C., Coldren, G., Berger, U., 2012. Investigating the role of impoundment and forest structure on the resistance and resilience of mangrove forests to hurricanes. Aquat. Bot. 97, 24–29.
- Walker, L.R., De Moral, R., 2003. Primary succession and ecossytem rehabilitation. Cambridge University Press, Cambridge.
- Webster, P.J., Holland, G.J., Curry, J.A., Chang, H.R., 2005. Changes in tropical cyclone number, duration, and intensity in a warming environment. Science 309, 1844–1846.Whelan, K., 2005. The successional dynamics of lightining-initiated canopy gaps in the

- mangrove forests of Shark River, Everglades National Park, USA. In: Biology. Florida
- International University, MIami, Florida, pp. 196. Whelan, K.R.T., Smith, T.J., Anderson, G.H., Ouellette, M.L., 2009. Hurricane Wilma's impact on overall soil elevation and zones within the soil profile in a mangrove forest. Wetlands 29, 16-23.
- White, P.S., Jentsch, A., 2001. The search for generality in studies of disturbance and ecosystem dynamics. In: Esser, B.K., Luttge, D.U., Kadereit, M.J.W., Beyschlag, B.W.
- (Eds.), Progress in Botany. Springer-Verlag, Berlin Heidelberg, pp. 399–449. White, P.S., Pickett, S.T.A., 1985. Natural disturbance and patch dynamics: an introduction. In: Pickett, S.T.A., White, P.S. (Eds.), The Ecology of Natural Disturbance
- and Patch Dynamics. Academic Press Inc, Orlando, FL, pp. 3-13.
- Zhang, K.Q., 2008. Identification of gaps in mangrove forests with airborne LIDAR. Remote Sens. Environ. 112, 2309–2325.
- Zhang, K.Q., Simard, M., Ross, M., Rivera-Monroy, V.H., Houle, P., Ruiz, P., Twilley, R.R., Whelan, K.R.T., 2008. Airborne laser scanning quantification of disturbances from hurricanes and lightning strikes to mangrove forests in Everglades National Park, USA. Sensors 8, 2262-2292.
- Zhang, K.Q., Thapa, B., Ross, M., Gann, D., 2016. Remote sensing of seasonal changes and disturbances in mangrove forest: a case study from South Florida. Ecosphere 7.